Development of a Prototype Kinestatic Platform for Application to Space and Ground Servicing Tasks

Phase I: Concept Modeling

Final Report

Submitted to:
J. Beeson
NASA Kennedy Space Center

by
J. Duffy & C. Crane
Center for Intelligent Machines and Robotics
University of Florida
Gainesville, Florida 32611

September 1993

Development of a Prototype Kinestatic Platform for Application to Space and Ground Servicing Tasks

Phase I: Concept Modeling

Final Report

Submitted to:
J. Beeson
NASA Kennedy Space Center

by
J. Duffy & C. Crane
Center for Intelligent Machines and Robotics
University of Florida
Gainesville, Florida 32611

September 1993

Foreword

The team consisting of the University of Florida, CC Mechanisms, and Rockwell International is pleased to present this report to NASA as a measure of the successful completion of the first phase of this project. In all projects involving the application of advanced technology to the solution of practical problems, there are several contributors which have provided inspiration and perspiration to the unqualified success of the project. We take time, here, to recognize these contributors.

Mr. Eric Rhodes, of NASA/KSC for his timely inputs and program guidance,
Dr. Michael Griffis, of CIMAR, for his tenacity and technical guidance in bringing the project to fruition,
Mr. Shannon Ridgeway, of CIMAR, for his excellent dynamic simulations,
Ms. Suzanne Hodge, of Rockwell International, for her program support and coordination effort,
Mr. Chris Larson, of Rockwell International, for his technical expertise and guidance in machining processes.

We look forward to continued cooperation with these individuals in phase 2 of this project in the coming fiscal year.

Dr. J. Duffy

Table of Contents

I. Project Goal and Technical Objective

The Center for Intelligent Machines and Robotics (CIMAR) of the University of Florida, in conjunction with Rockwell International is developing an electro-mechanical device called a Kinestatic Platform (KP) for aerospace applications. The goal of the current project is to develop a prototype KP which is capable of manipulating a 50 lb. payload. This prototype will demonstrate the feasibility of implementing a scaled up version to perform high precision manipulation of distributed systems and to control contact forces and allowable motions (rotations and translations), which is defined here as Kinestatic Control, in a six dimensional, partially constrained environment, simultaneously and independently.

The objectives of the Phase I effort were as follows:

1) Identify specific NASA applications where the KP technology can be applied.
2) Select one application for development.
3) Develop a conceptual design of the KP specifically for the selected application. This includes the steps of developing a set of detailed performance criteria, establishing and making selection of the mechanism design parameters, and evaluating the expected system response.
4) Develop a computer graphics animation of the KP as it performs the selected application.

This report will proceed by providing a technical description of the KP followed by how each of these objectives was addressed.

II. Background - Technical Description of Kinestatic Platform

A "platform" or "parallel mechanism" is defined as any mechanical device that has six legs that connect a moving platform to a base. This kind of mechanism possesses the desirable characteristics of high accuracy, high payload-to-weight ratio, and good static stability. In order to apply Kinestatic Control to such mechanisms it is necessary to first obtain accurate compliance models. These models can be readily determined for parallel mechanisms, provided that the position and orientation of the moving platform is known relative to the base. Therefore, the key and central task is to determine the

position and orientation of the moving platform relative to the base given the sensed lengths of the six legs. This task is referred to as the forward kinematic analysis for the system, and for these kinds of mechanisms the simplest solution involves solving an eighth degree polynomial in a single variable.

The geometrically simplest parallel mechanism has the structure of an octahedron, and it is designated as a "3-3 platform" since there are three connecting points on the base and three on the moving platform. The double connection points shown in Figure 2.1 produce a very simple geometry. However, there is a very serious mechanical disadvantage. It is not possible to design the necessary concentric ball and socket joints at each of the double connection points without significant mechanical interference. It is preferable to separate the double connection points and in this way to overcome the mechanical design problem.

In general, as double connecting points are separated, the complexity of the forward kinematic analysis for the platform increases. It should be noted that there are multiple solutions. This means that there are multiple closures of the mechanism and that there exist a number of different ways it can be assembled. Each assembly yields a different position and orientation of the platform for a given set of six leg lengths.

It is, of course, possible to perform numerical iterations (an optimization using six independent variables) to obtain the position and orientation of the platform. However, it is well known that such iterative solutions have a tendency to "jump" from one closure to another. From a practical viewpoint, this is undesirable. It is far more desirable to derive a single polynomial in a single variable, the solution of which yields all possible locations of the moving top platform. The desired solution can then be extracted from this finite set of all solutions. Such a solution is said to be in "closed-form".

It was only recently that the closed-form forward analysis for the geometrically simplest 3-3 platform was solved by Griffis and Duffy [1]. Briefly, an eighth degree polynomial solution was derived, and this has been extended to a 6-3 platform (Stewart's original platform [2], see Figure 2.2). It would be desirable to perform the forward analysis for a general 6-6 device as shown in Figure 2.3, however this is unrealistic. The closed form equation will be at least a 40th degree polynomial, which has been obtained for a similar device of lesser complexity [3], and this is computationally impractical for real time control. Griffis and Duffy have invented two platforms which provide the benefits of

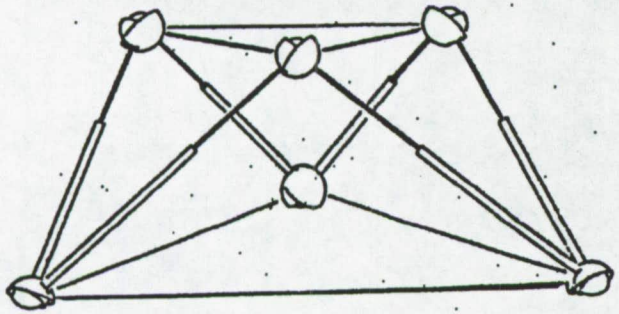

Fig. 2.1: 3-3 Platform

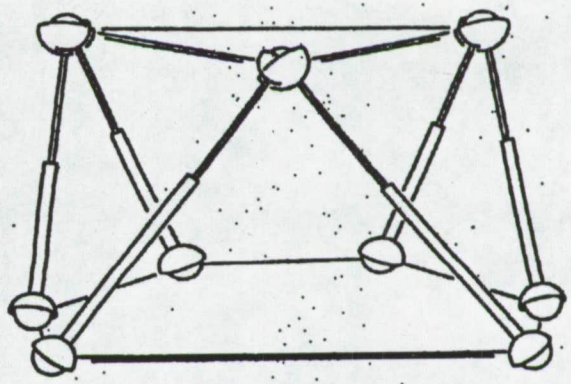

Fig. 2.2: 6-3 Platform

Fig. 2.3: 6-6 Platform

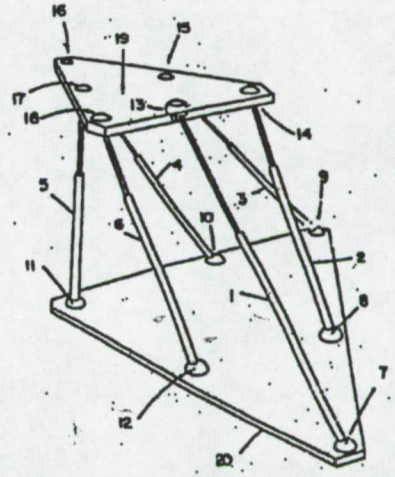

Fig. 2.4: Special 6-6 Platform

both the 3-3 and general 6-6 platforms. These platforms, which have been patented by the University of Florida, allow for the simple analysis of the 3-3 with an eighth degree polynomial, and allow for the mechanical benefits of the general 6-6 by eliminating mechanical interference. One of these new platforms is shown in Figure 2.4. A table mounted model KP has been fabricated and this is shown in Figure 2.5.

As previously stated, the necessity for a simplified closed-form forward kinematic analysis (specialized geometry) manifests itself whenever the mechanism is to control force and position simultaneously. The requirements of specialized geometry and good mechanical design (no mechanical interference) is satisfied by the platforms that have been patented by the University of Florida. It is the union of the theory of Kinestatic Control [4][5] and these platforms that yields the KP concept.

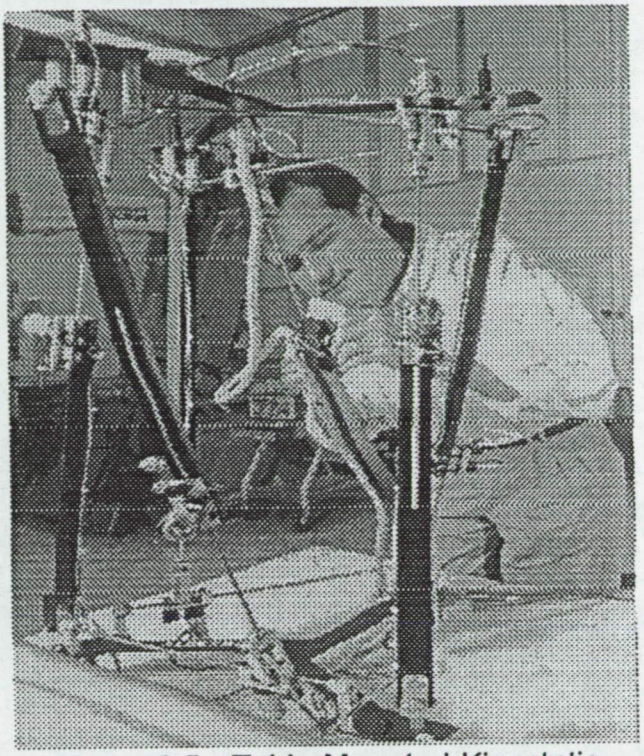

Figure 2.5: Table Mounted Kinestatic Platform

III. Identification of Applications

The ability of the KP to accurately and simultaneously control position and force is one of the properties that distinguishes the device from conventional robotic mechanisms. This capability allows the KP to be utilized in a wide variety of new applications. Several of these applications have been identified as part of the Phase I effort and are discussed in this section of the report.

A. Solid Rocket Booster (SRB) Alignment - Ground Handling Support Equipment

SRB alignment is a critical process which is performed as an integral part of the overall shuttle launch preparation process. In this process, the longitudinal axes of the SRB's are aligned with the remaining launch package during the stacking process in the Vertical Assembly Building (VAB). Because the process is sensitive to external vibrations, and because the day shift actively produces undesirable vibrational input, the SRB alignment process is, by force of necessity, relegated to the third shift when vibrations are at a minimum. The implementation of a KP-based alignment structure obviates the need for selective shift SRB alignment by virtue of the fact that it can be used to filter out undesirable external vibrations during the alignment process. In this application, the KP is used as a random or periodic disturbance input filter.

Currently, the simultaneous alignment of the four hold-down posts with the forward disconnect assembly is performed by precise laser alignment procedure. A platform employing the KP technology could isolate equipment from the surrounding vibrations resulting in the following benefits:

- reduced alignment time
- reduced manpower
- shift flexibility (enables operations to be conducted on first or second shift).

B. Engine Installation and Removal

A KP-based device can be used effectively in applications which require precision control of a distributed mass with respect to a specific orientation in inertial space. This is a unique application whenever the movable platform is not always free to move and is required to come into contact with the environment. In such a case, it is essential that the top platform be capable of controlling or limiting the magnitude of the external contact force that is applied to the top platform. As a relevant application to the shuttle, consider the case where a shuttle ground support crew must remove or replace an engine. The

KP can be employed as a three-dimensional or spatial jack where the movable platform manipulates the engine for removal or insertion. It is essential not only to control allowable motion but also to avoid damage by controlling forces and couples simultaneously when the engine comes in contact with the shuttle wing or fuselage. The issue of simultaneous control of force and motion is critical to this operation.

The present process for installing the shuttle main engines is a meticulous, time-consuming, and manpower-intensive process. It is a logical extension of the characteristics of the KP platform to use it for precise manipulation of the engines, including removing of the engines on the pad, if necessary. In the latter instance, a KP-based engine manipulator will reduce the effort associated with an engine swap out and will minimize any additional realignments.

Currently four work shifts are required to install an engine with a one-of-a-kind tool. This tool, the Hyster, has a specialized grapple. Since it is not economically feasible to purchase a second grapple for the shuttle program, a backup part does not exist. The KP offers a solution without the constraint of having to conform to specific engine dimensions. Additionally, the KP can be designed to have multiple utility for different distinct applications throughout the assembly process. The KP will, in fact, minimize logistic requirements by replacing a specialized tool with a multipurpose tool (KP) and optimize tool usage within the facility.

C. Payload Installation and Removal

The KP provides a solution to the problems associated with operations in which a distributed mass must be rotated or translated in inertial space in a 6 D.O.F./constraint environment. More specifically, the KP can be used to install and remove payloads under constrained environmental conditions and can be designed to accommodate a wide dynamic range of payload weights and weight distributions.

The cost of platform development for the payload manipulation application is directly related to the weight of the payload being manipulated and to the distribution of the payload weight within the physical envelope of the payload itself. A properly designed KP-based platform with sufficient capacity can be a cost-effective device since this technology is sufficiently flexible to accommodate a wide variety of payload installation

and removal tasks. Consequently, it is recommended that the requirements for the life sciences flight manifest for 1994/1995 be investigated for potential KP platform applications.

D. Gyro's, IMU's, Shuttle Controllers

The calibration and/or alignment of gyroscopes, IMU's, and Shuttle Controllers are sensitive operations requiring precision processes and are candidate applications of KP technology. Gyroscope calibration is executed within the KSC Shuttle Depot Activities Shop and utilizes 7'x7'x1' concrete slabs in order to isolate the gyro from random or sinusoidal motion input. A KP-based calibration apparatus approximately 30 lbs. in weight will obviate the need for the massive concrete slabs.

IMU and Shuttle Controller calibrations are also promising candidates for KP-based technology applications. At present these are calibrated at vendor facilities. KP-based technology can provide the precision necessary to perform the calibrations in house. This can reduce costs as well as turnaround time. As a first step in the overall process, this report recommends the identification of all equipment calibration which can benefit from the commonality approach suggested here.

E. Machine tool-grinder

GSE and Flight Hardware require precision ground surfaces. Parts for such hardware call for exacting requirements on flatness, contour, close tolerance, or surface callouts. Also, grinding of compound angles is difficult and time consuming. A KP-based application can address this challenge by virtue of the flexibility afforded by its software. For example, there exist requirements for grinding three-way solenoid valve surfaces. Because the valves are tapered, a time consuming setup is involved. This setup time is drastically decreased using the KP tool. A small scaled version of the platform can be mounted securely to the grinder work table, thereby positioning parts to be ground. This expands the machine capability by allowing it to effectively operate with 6 degrees of freedom.

Specialized nuts, bolts, and screws require a grinder operation with rotation about the X, Y, Z axes. These are small parts where the weight factor is less than a pound and precision is required for special threads. Cost can be reduced if these parts are made locally within the NASA Shuttle Logistics Depot Machine Shop. The same platform used to address the valves can be scaled to meet the needs of grinding many small parts.

F. Machine tool-mill

Although the NASA Shuttle Logistics Depot possesses two-axis vertical milling capability, there exist also requirements for 5-axis milling of shuttle parts. Currently 5-axis milling is contracted to offsite vendors and is estimated at over 1.9 million dollars per fiscal year. The implementation of KP technology will enhance current milling capacity to 5-axis milling capability and will reflect the following benefits:

- Annual savings of approximately $600K per year
- Reduced turn around time on parts
- Improved finish on machined parts
- Expansion of existing machine capability.

G. Machine tool-Horizontal boring Mill

The existing horizontal boring mill located at the NASA Shuttle Logistics Depot is used for fabricating large ticket items such as the fabrication of GSE platforms and for the modification of the keel ridge. The utility of this machine can be expanded to other functions such as the fabrication of spherical tanks which are currently manufactured at a vendor site. The enhanced capability is accomplished by retrofitting this machine with a kinestatic platform modification which will give it the ability to manipulate bulky items.

A low risk approach to development costs associated with the recommended retrofit consists of incremental development of functionally similar but lower capacity

equipment. Application of this technology to the grinder or 2-axis vertical mill will provide proof of concept and operation with minimized development cost expense. Upon successful completion of this development, KP-based technology will be considered for the larger capacity horizontal boring mill application.

H. Machine tool-lathes

Several types and sizes of lathes exist in the NASA Shuttle Logistics Depot. The platform can expand the usage of the lathes to a CNC lathe. Cutting tools can be mounted to the platform table generating precise tool paths. Bowl type items and unique contours can be generated with the use of the platform. All lathes within the depot appear to be candidates for this technology.

A platform which is sized to meet the needs of grinding can also meet the needs of the lathe operations. This interchangability characteristic allows the cost of development to be spread to multiple functions and, consequently, improves the payback.

I. Specialized Jigs for Part Installations

The shuttle program has responded, as needed, to specific requirements by fabricating specialized jigs. One such specialized rig is used in the installation of the shuttle window glass into the window frame molding. The proper installation procedure requires that the seal be secure and the glass be lowered into the frame precisely so that pressure on the glass is distributed uniformly along the entire frame of the molding. The jig that was developed for this specific task works extremely well. However, this GSE can only be used for one specific purpose, shuttle window glass installation. A KP-based, multifunctional GSE can reduce total life-cycle costs since it can replace several specialty equipment with one KP-based multiple-utility GSE.

J. Future Programs - Stable Platform for Space Assembly Operations

A preliminary assessment of the characteristics of the KP suggests that it not only has enhanced performance capability for existing operations but also shows promise in

meeting the requirements of future missions. Two such missions which can benefit from KP-based technology are Space Station Freedom (SSF) assembly and operations and the Assured Crew Return Vehicle program. In the former case, the KP platform can be an integral and effective part in the process by which the SSF structural elements are manipulated into position for attachment to other structural elements. The unique ability to maintain a precise orientation in inertial space and to filter out undesirable disturbance forces is critical to rapid and efficient assembly of the station structural elements.

In the area of periodic scheduled maintenance, as well as preventive maintenance on SSF, the KP can be used to execute cleaning functions as well as LRU replacement in areas which are not accessible to the crew or which require high mechanical advantage for removal or replacement.

The ACRV program mission is the safe return of SSF astronauts in the event of an impending catastrophic event, serious astronaut illness, or a request to evacuate SSF for other reasons. A crew member that is either injured or has experienced an extended stay in a zero-g environment will require assistance because of a diminished capacity to interact in a 1-g environment. This assistance can be achieved with a KP-based device which will facilitate the negotiation of the deconditioned crew member from a water-lander or from a land-lander in rough terrain.

K. Cleaning Operations

In the application depicted in Figure 3.1, the standard PUMA manipulator is retrofitted with a kinestatic platform (KP), enabling the platform to serve as a "wrist", to accomplish various cleaning operations when various end effectors are mounted to the end of the platform. The kinestatic platform must be designed to interface with the existing PUMA robot technology and be adaptable to various solutions for end effectors. The kinestatic platform serves as a direct interface plate to the end effector and is able to perform repetitious operations on a round-the-clock basis.

Cleaning operations are fundamental to the effective and efficient operation of the O&C, VAB, and VPF facilities. These operations range from cleaning of sensitive control panels onboard SSF to cleaning of Shuttle radiators and payload canisters. It is reasonable to expect that a single end effector design can accomplish most cleaning

operations. At present, however, the KP-based precision cleaning assembly (PCA) application is intended to address the challenge of removing dust and fiber particles, grease, and oil from instrument panels containing buttons, knobs, dials, switches, safety chains, and video screens. In addition, it will be used to clean spherical surfaces and payload canisters.

The present scheme for cleaning Shuttle radiators involves a manual, time-consuming process accompanied by the use of bridge buckets. A KP-based, autonomous cleaning capability reduces the risk associated with hazards to personnel and equipment, minimizes operational time, and minimizes operational costs involved in the operation. Safety is a driving factor and serves as the catalyst in this cleaning application development.

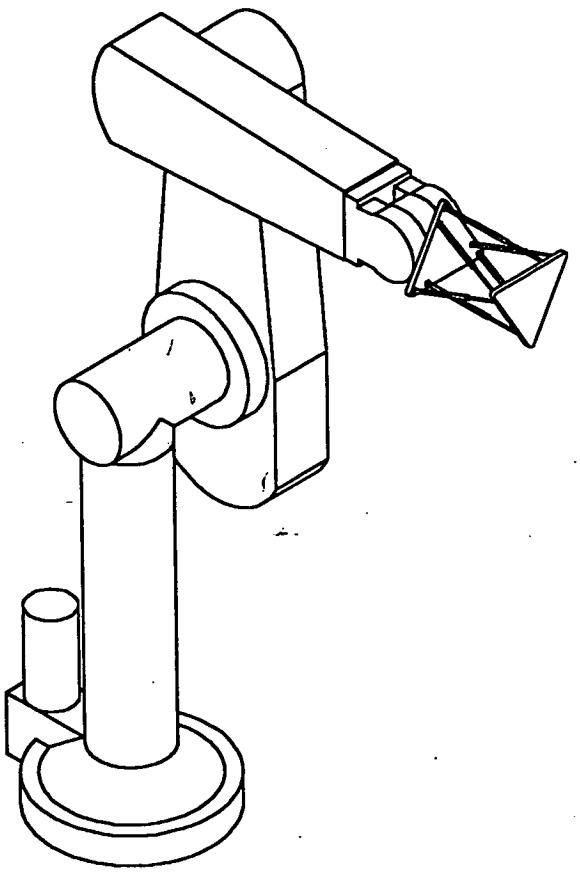

Figure 3.1: Puma Robot with KP Attached

The KP can provide a solution to these cleaning challenges. However, further investigation is needed to determine the following:

- The type of end effector that meets the requirements of radiators, panels, and canisters.

- Residue must be defined for each cleaning task. Panels that reside in a 100K clean room do not have the same residue/cleaning requirements as the shuttle radiators. Canisters require further cleaning requirements to be defined.

IV. Selection of Application

A. Specific Application

It is recommended that the milling operation identified in section III.F. be pursued as the first application for the KP. This recommendation is based upon (1) the potential immediate impact on operations (cost and schedule) and (2) the mitigation of risk. The performance requirements needed for this application are not as exacting as those associated with other potential applications. The scope of the milling operations requirements will minimize the cost of development.

B. Definition of Demonstration Success

In order to minimize development risk, and in order to address current and future program needs, the following demonstration project was formulated. The KP will be used to augment an existing 2-axis vertical mill in order to expand the local capability at the depot to fabricate parts that currently cannot be manufactured on site.

Several parts were considered as candidates for the demonstration. The following three parts were selected:

- Fitting, V070-353258 (see Figure 4.1). This fitting is a member of the main structure frame and it is located in the aft section of the orbiter. Two of these parts are required for each orbiter.

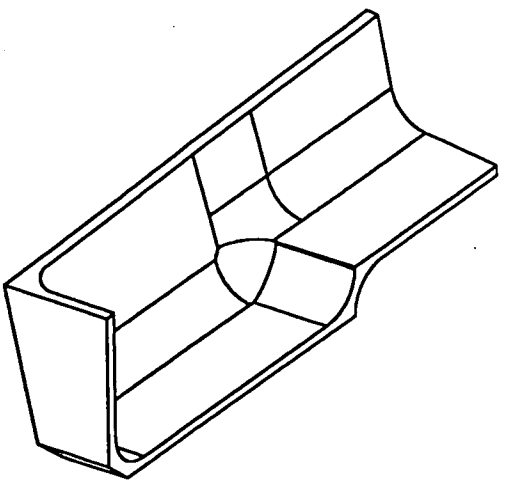

Figure 4.1: Fitting

- Flow Sensor Boss, V070-382156 (see Figure 4.2). The boss is located in the forward fuselage. This component is directly bonded to a fitting. The fitting part number is V070-382145-001. The boss houses a flow sensor to measure the flow of air in the compartment.

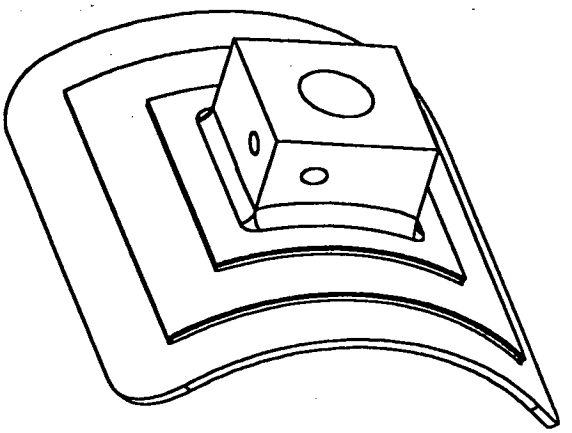

Figure 4.2 Sensor Boss

- Shell, V070-855061 (see Figure 4.3). The shell is bolted to the orbiter and is used to connect the external tank to the orbiter. There are two shells on each orbiter in the aft section. The shell and the monoball act as a ball and socket. The monoball rides on a substance called Kahrlon inside the shell. The monoball is connected to the external tank and mates into the shell. The shell bolts to the monoball by an explosive nut. This explosive nut discharges and separates the orbiter from the external tank.

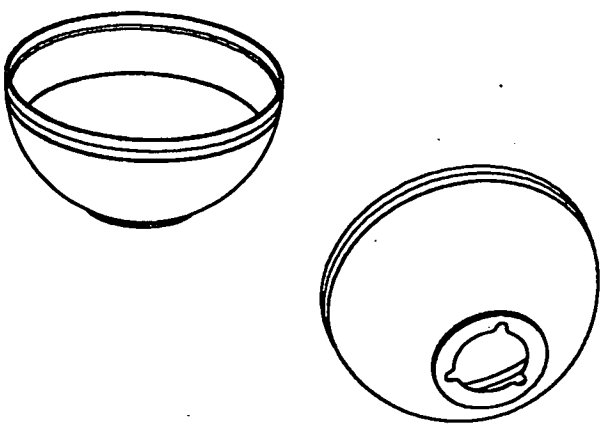

Figure 4.3 Shell

C. Program Needs / Costing Identification

The development program has been divided into three sections. Phase I, which is complete, and is the substance of this report, consisted of identifying applications for the KP and presenting a conceptual design. Phase II will entail prototype development. Phase III will deal with system integration and demonstration. The funding required for these three phases is presented here.

Phase 1

Labor Category	Hours	Rate/Hr.	Cost	
Graduate Research Prof., J. Duffy	21	$64.62	$1,357	
Assistant Prof., C. Crane	21	32.42	681	
Post Doc., M. Griffis	416	20.10	8,362	
Research Assistant (1)	260	12.80	3,328	
				$13,728
Fringe Benefits				
salaried employees: 25.5% + $228 per man month			$575	
post doc.: 8.3%			694	
				1,269
Expenses				
Subcontract - Rockwell			$19,720	
Software			420	
Postage, telephone, copies, etc.			489	
				20,629
Travel				
Demonstration at KSC (3 persons, 2 days)				
Lodging ($60 per night)			$180	
Rental Car			150	
Per Diem ($21/day per person)			126	
				456
TOTAL DIRECT COSTS				$36,082
INDIRECT COSTS				
43% of Total Direct Costs				15,515
Permanent Equipment				
None			$0	
				$0
TOTAL BUDGET REQUIRED				$51,597

Phase 2, 1 Oct 93 - 30 Sep 94

Labor Category	Academic Year	Summer	Hours	Rate/Hr.	Cost	
Graduate Research Prof., J. Duffy	10%	10%	208	$66.81	$13,896	
Assistant Prof., C. Crane	10%	10%	208	33.54	6,976	
Post Doc., M. Griffis	75%	75%	1560	20.10	31,356	
Technician	20%	20%	416	14.00	5,824	
Research Assistant (1)	33%	35%	704	13.00	9,152	
Research Assistant (1)	50%	50%	1040	5.25	5,460	
						$72,664
Fringe Benefits						
salaried employees: 25.5% + $228 per man month					$7,902	
post doc.: 8.3%					2,603	
						10,505
Expenses						
Subcontract - Rockwell					$75,467	
Racks (6)					600	
Gears (used on motors) (12)					144	
Gears (used on sensors) (24)					288	
Shaft Collars (24)					168	
Ball Bearings (6)					120	
Thrust Bearings (6)					180	
Steel Material					500	
Bushings (24)					120	
Power Supply					600	
Encoders (12)					624	
Leg Force Sensors (6)					600	
Misc. Hardware (Fastners, potentiometers, etc.)					2,500	
Misc. Electronics (Prototype computer data cards)					3,000	
Fabrication shop time (600 hours @ $30/hr)					18,000	
Computer Software					2,100	
Motor Control Cards					10,000	
						115,011
Travel						
Demonstration at KSC (3 persons, 2 days)						
Lodging ($60 per night)					$180	
Rental Car					150	
Per Diem ($21/day per person)					126	
						456
TOTAL DIRECT COSTS						$198,636
INDIRECT COSTS						
44% of Total Direct Costs						65,194
(44% of 1st $25K of subcontract)						
Permanent Equipment						
Force/Torque Sensor					$6,500	
Motors and Amplifiers (6)					24,000	
Ball Screws (6)					3,000	
486 Industrial Computer					10,000	
						$43,500
TOTAL BUDGET REQUIRED						$307,330

Phase 3, 1 Oct 94 - 31 Mar 95

Labor Category	Hours	Rate/Hr.	Cost	
Graduate Research Prof., J. Duffy	156	$66.81	$10,422	
Assistant Prof., C. Crane	208	33.54	6,976	
Post Doc., M. Griffis	1040	25.00	26,000	
Technician	208	14.00	2,912	
Research Assistant (1)	343	13.00	4,459	
Research Assistant (1)	520	5.25	2,730	
				$53,499
Fringe Benefits				
salaried employees: 25.5% + $228 per man month			$5,931	
post doc.: 8.3%			2,158	
				8,089
Expenses				
Subcontract - Rockwell			$37,411	
Office Supplies			1,000	
				38,411
Travel				
Demonstration at KSC (3 persons, 2 days, 2 trips)				
Lodging ($60 per night)			$360	
Rental Car			300	
Per Diem ($21/day per person)			252	
				912
TOTAL DIRECT COSTS				$100,911
INDIRECT COSTS				
45% of Total Direct Costs				39,825
(45% of 1st $25K of subcontract)				
Permanent Equipment				
None			$0	
				$0
TOTAL BUDGET REQUIRED				$140,736

V. Development of Conceptual Design

Phase 1 of this conceptual effort consists of the development of a conceptual design which incorporates a KP as an integral and distinct element of a specific application: light 5-axis contour milling.

A. Design Specifications

As a rule, when designing a KP, the anticipated application must be considered. The application defines loadings, workspace geometry and dexterity. The specific application for which a KP is being developed is 5-axis contour milling. Several assumptions are made with regards to this application:

1. An existing 2 hp Bridgeport milling head will turn the cutter.
2. Aluminum will be the working material.
3. Part geometry is restricted in scale.

Parts to be fabricated with the KP have been selected from a group that cannot be easily machined within the capacity of NASA Logistics Depot. Three candidate parts are shown in Figures 4.1 through 4.3. Figure 4.3 shows a shell that is used to connect the external fuel tank to the orbiter. It is the largest expected part and is used to establish the boundaries of the geometric workspace of the KP.

Workspace definition

The geometric workspace is defined by the work volume of the shell. Figure 5.1 shows the volume necessary to mill the shell using a reasonable cutter (1 inch diameter).

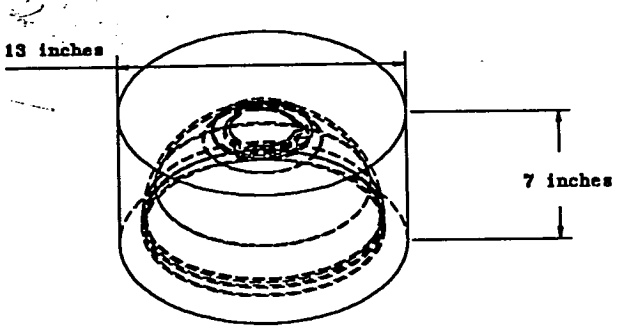

Figure 5.1: Workspace Geometry

Force and Velocity Definition

The determination of the cutting force and velocity associated with a particular milling operation is of paramount concern insofar as the quality of the product is concerned. It is the intent of this section to present the analysis relative to the determination of the former (velocity determinations are presented in subsequent sections). The nomenclature used in the analysis is presented as follows:

b ==> chip width, mm,
typically < .2 mm

h_1==> undeformed chip height, mm,
typically < 5mm

k_s==> cutting stiffness, N/mm^2,
empirically determined.
For aluminum, k_s = 850 N/mm^2

F_t==> tangential force, N

F_n==> normal force, N (typically approximately .3×F_t

Conventional mills are serial chains of cartesian joints involving complex forces and the transmission of these complex forces across joints and interfaces. These complex forces have normal and tangential components which are of major significance in the design of conventional milling machines. The integrity of the contour of the finished, milled product is a sensitive function of the degree of control of these normal and tangential components at the cutting interface. The KP provides the required degree of

control with respect to the latter. The differential of the cutting stiffness allows the tangential cutting force to be determined explicitly by:

$$F_t = b\, h_1\, k_s \qquad (5.1).$$

For typical chip geometry, equation 5.1 yields,

$$F_t = 5 \times 0.2 \times 850 \text{ N} = 850 \text{ N} = 191 \text{ lbf.}$$

The normal force has been empirically determined to be approximately $.3 \times F_t$ for typical milling operations. In summary, then, the magnitude of the active load can be determined from the relationship:

$$F = (F_t^2 + F_n^2)^{1/2} = 1.044 \times F_t \qquad (5.2)$$

where, for a typical chip geometry, $F \approx 199.4$ lbf. This load is considered to act at any point in the geometric workspace and at any spatial orientation.

Another load of interest to the designer of a precision milling machine is the inertial load of the mass of the workpiece. The upper limit of this mass is set as that mass of material which would occupy the entire workspace. Using aluminum as the working material, this mass is given by:

$$m = \Pi \times r^2 \times h \times \rho \qquad (5.3)$$

$r = .1651$ m

$h = .1778$ m

$\rho = 2800$ kg/m^3

Consequently, $m = 42.63$ kg.

The velocity range necessary to effectively mill the work material is established by the capacities of the existing milling head and on current milling practices.

Feed rate along the specified cutting path needs to be constant.

Minimum feed rate of .2 cm/min (.1 ipm)

Maximum feed rate of 60 cm/min (23.6 ipm)

B. Identification and Establishment of Mechanism Design Parameters

The kinestatic design of a KP-based milling application is based on a structured top-down methodology. This methodology consists of establishing a minimum set of design variables and of establishing a baseline design as well as alternate concepts based upon system level requirements. The candidate design (baseline plus alternates) is then evaluated against specific operational requirements of the application (cutting force, velocity, frequency of the actuator). Since the actuator and KP must work in concert, and since the actuator dynamics impact the overall system dynamics, a tentative, parametric process is implemented in order to achieve a final optimal operationally-sensitive design.

Kinestatics:

The general KP's kinematics can be described parametrically by defining two triangles, the base and the top, and six side pivot connections. The base and top triangles need not be equilateral or symmetric. Because the expected loading is arbitrarily placed in the workspace, the KP manipulator should exhibit as uniform a stiffness and response over the workspace as possible. This design specification leads to equilateral triangles for the base and top. The position of each connecting pivot should be symmetric on each triangle, but need not be the same for the base and top.

An equilateral triangle can be defined with one parameter. We choose the side length as this parameter. Figure 5.2 is an illustration of the parameterized kinematics. The base triangle is defined by the parameter *side*. The top triangle is related to the base triangle by the parameter *tbscale*. The base side pivot positions are defined by the parameter *bscale* and the top side pivots positions are defined by the parameter *tscale*.

The special 6-6 parallel mechanism requires that the pivot connection lie on the line that contains the two vertex connections. For example, in figure 5.2, side pivot connection s_o must lie on the line that contains o_o and p_o. The parameters *bscale* and *tscale*, along with the parameters *side* and *tbscale*, are used to establish the position of the side pivots as shown in figure 5.2. On the base, if *bscale* is less than 1, then the side pivot lies between the two vertex connections. If *bscale* is greater than 1 then the side pivot lies outside the vertex connection points. The same is true for *tscale*, with respect to the top. These four parameters permit the kinestatic examination of candidate KP manipulators for a given application. The static stability of the KP over its range of operations requires detailed analysis. This stability will be a function of the design of the individual system elements which constitute the overall system and especially of the required performance of the top platform as it is commanded to traverse the workspace within physical and temporal operational constraints. The parameter *side* allows the mechanism to be scaled up or down. The parameters *tbscale, tscale* and *bscale* define the kinematic workspace and variation of static stability across the kinematic workspace. The kinestatic design methodology consists of finding suitable *side*, *tbscale, tscale*, and *bscale* that define a KP that has well behaved static stability over a workspace and that meets the design specifications.

Static Stability

There exists a relationship between the forces at the top platform and the forces in the actuators of a parallel mechanism. This relationship is called the jacobian and is defined by:

$$F_c = F_{actuators} \times j_c \qquad (5.4)$$

where:

F_c ==> external contact force/couple at platform

$F_{actuators}$ ==> forces in the actuators

j_c ==> linear transformation which varies with mechanism's position and orientation

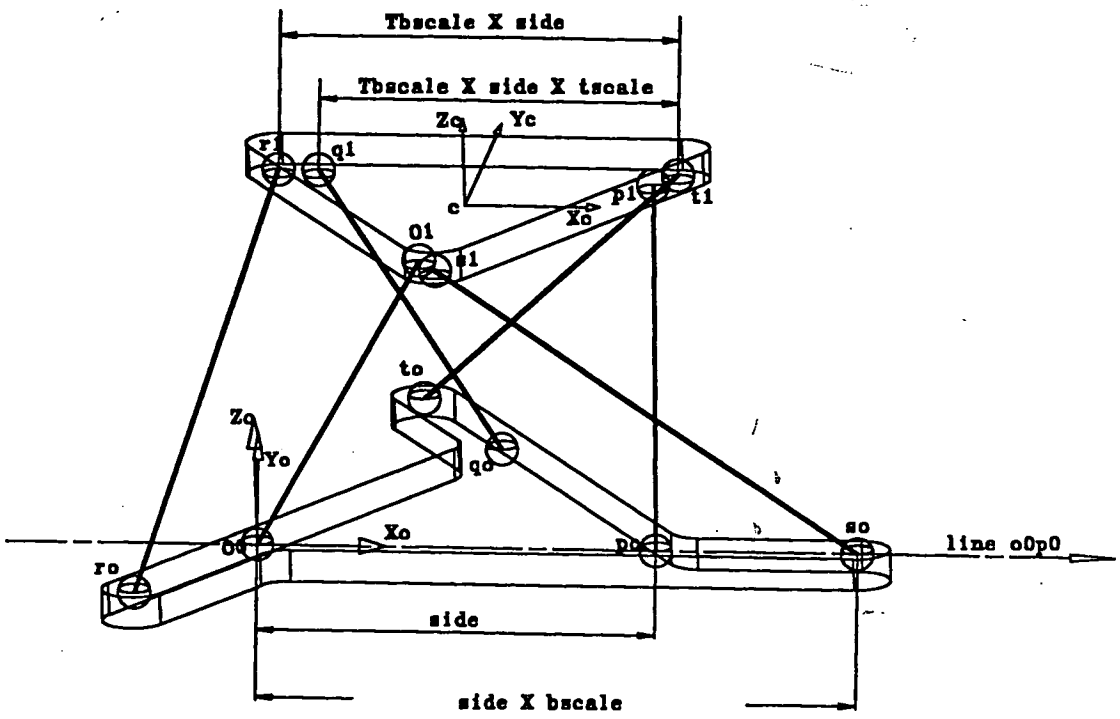

Figure 5.2: Kinematic Parameterization of KP.

The numerical value of the determinant of j_c for a given set of kinematic parameters is a measure of the relative stability of the system. There are, in fact, mechanism configurations wherein there is no ability to exert a load in a certain direction. These prohibited directions are called singularities. This occurs when the determinant of j_c is zero. It is therefore imperative that there exist a mathematical methodology in the form of an algorithm that can constantly manipulate a large order square matrix (the determinant of j_c) and obtain a numerical value for that determinant. Such an algorithm has, in fact, been developed. The actual value of the determinant is not as important as the rate of change of the determinant as the workspace of a candidate mechanism is traversed. The results of this procedure give some indication of the mechanism's stability (stiffness) over it's workspace.

Examination of candidate mechanisms is carried out by selecting the four mechanism parameters *side, tbscale, bscale*, and *tscale*, and evaluating the determinant of the jacobian over the mechanism's workspace. The algorithm first finds the nominal

position, that is, the position in which the determinant of the jacobian is greatest. Then the nominal position and orientation can be defined as the frame at the center of the top platform with orientation parallel to frame zero that generates the maximum determinant of the jacobian. To examine static stability, the algorithm evaluates the determinant of the jacobian while varying position and orientation about the nominal position. Results are presented in a normalized fashion using the maximum determinant of the jacobian for each case.

Details of each case are presented, defining parameters and reporting nominal positions. Selected results are presented in the following figures.

Case a:
side = 1.000, Tbscale = 1.000, bscale = 1.500, tscale = 0.800
Nominal position:
orientation of c: roll = 0.00 pitch = 0.00 yaw = 21.78
position of c: x = 0.5000 y = 0.2887 z = 0.6834
maximum det[j] = 0.769129
leg lengths:
leg[1] = 0.8903 leg[2] = 1.0704 leg[3] = 0.8903
leg[4] = 1.0704 leg[5] = 0.8903 leg[6] = 1.0704

Case b:
side = 1.000, Tbscale = 1.000, bscale = 0.800, tscale = 0.800
Nominal position
orientation of c: roll = 0.00 pitch = 0.00 yaw = 0.18
position of c: x = 0.5000 y = 0.2887 z = 0.4157
maximum det[j] = 0.589711
leg lengths:
leg[1] = 0.5893 leg[2] = 0.5874 leg[3] = 0.5893
leg[4] = 0.5874 leg[5] = 0.5893 leg[6] = 0.5874

Figures 5.3 and 5.4 show the variation of the determinant of the jacobian as position and orientation is varied along a single dimension about the nominal position.

Figure 5.5 shows the change in leg length for change in roll for case a. Figure 5.6 shows the change in leg length for change in x for case a. Figure 5.7 shows, for case b, the change in leg length for change in roll. Figure 5.8 shows the change in leg length for change in x for case b. All leg lengths are normalized with respect to side length.

The parametric examination techniques developed here will be used in Phase II of the project to help determine the values for the parameters *side*, *tbscale*, *bscale*, and *tscale*. Determination of these four parameters will in effect complete the geometric design of the KP.

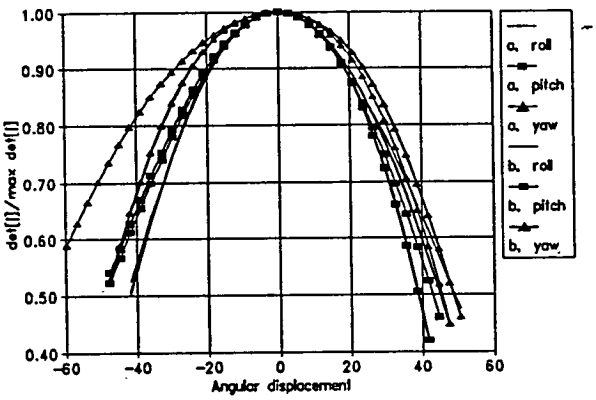

Figure 5.3

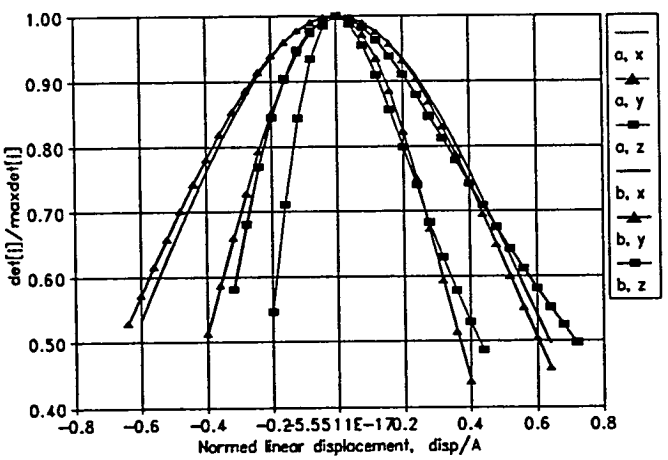

Figure 5.4

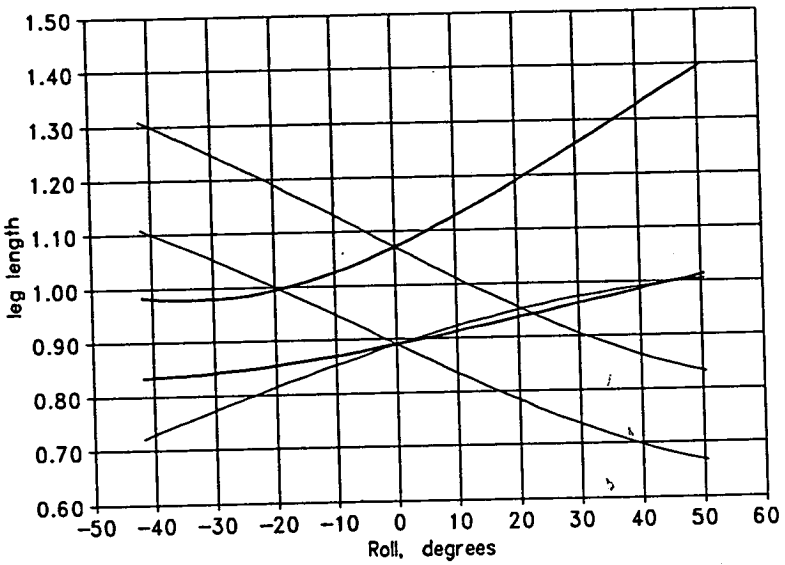

Figure 5.5: Case A, Rotation about the Roll Axis

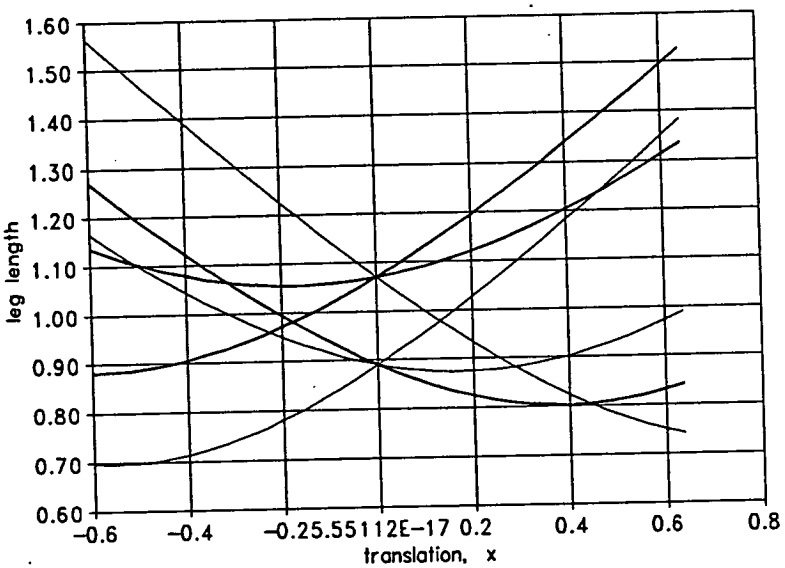

Figure 5.6: Case A, Translation along the X Axis

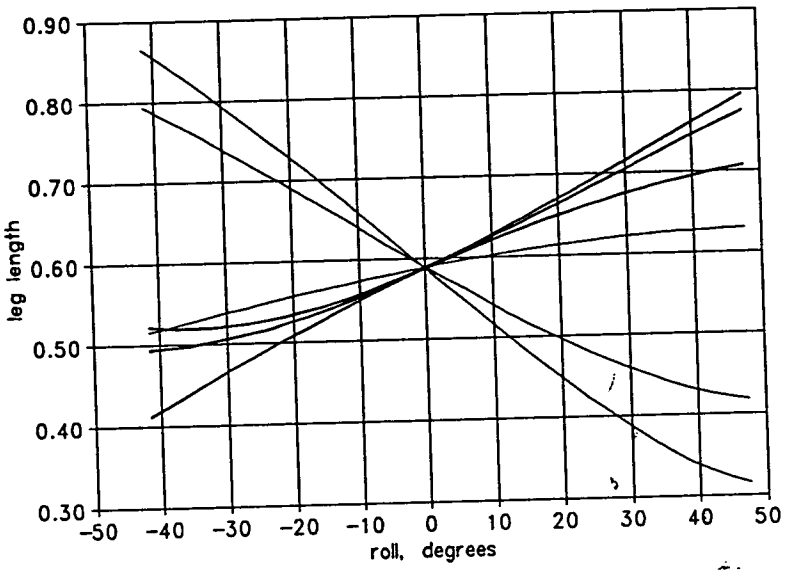

Figure 5.7: Case B, Rotation about the Roll Axis

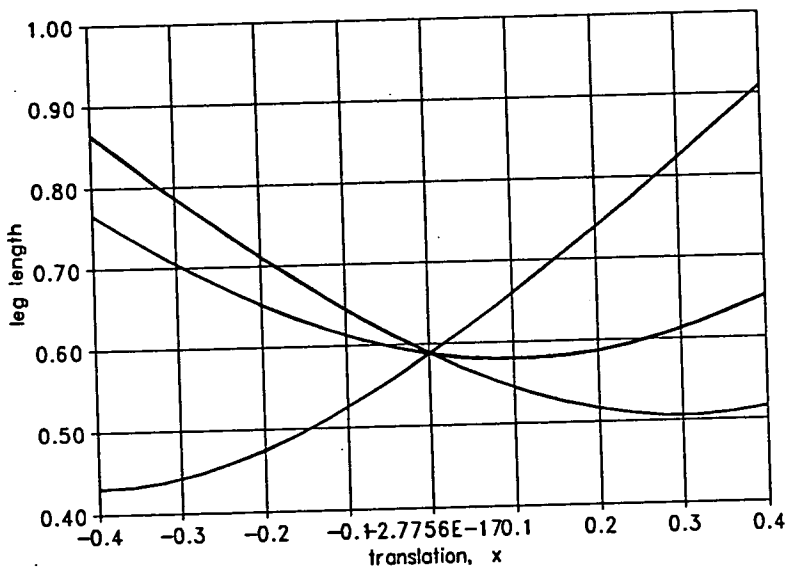

Figure 5.8: Case B, Translation along the X Axis

C. Dynamic Modeling and Control

The following is an analysis of the dynamic response of the kinestatic platform. The analysis investigates a single leg and includes the effects of the controller. The results of this preliminary assessment are promising and show that the platform can be successfully applied to a milling operation.

For a milling-type operation, it is essential that a disturbance force be included at the outset. This disturbance force is primarily applied by the milling cutter, and the result of too much disturbance force is called "chatter", which is a beating phenomenon that adversely affects the position control of the workpiece.

The approach taken here to avoid chatter is novel. It consists of both active and passive components in the kinestatic platform. First, for disturbance forces of lower frequencies, the actuator force will be used to actively provide the equal and opposite force to nullify disturbance effects. Secondly, for disturbance forces of higher frequencies, a "de-coupling" damper is employed to passively maintain the length of a given leg.

In addition to the disturbance and actuator forces and de-coupling damping, the dynamic modelling of the platform is based upon the magnitude of the masses, coupling damping, stiffness, and gear-train parameters. (In order to obtain the minimal set of dynamic modelling parameters, the equations have been simplified to three dimensionless parameters [mass ratio and 2 damping ratios].) Two transfer functions relating the velocity of the workpiece to the disturbance force, and the velocity of the workpiece to the actuator force are derived and compared for various sets of design parameters. It is the purpose of this exercise to demonstrate that the active/passive scheme allows for the control of disturbance forces (chattering) over the entire frequency spectrum.

Figure 5.9 introduces the notation that will be used throughout for the single leg analysis. The nomenclature is as follows:

x -- absolute displacement of end of leg

y -- absolute displacement of nut

θ_m -- rotation of motor

θ_s -- rotation of screw

m_a -- reflected platform mass (effective platform mass on leg)

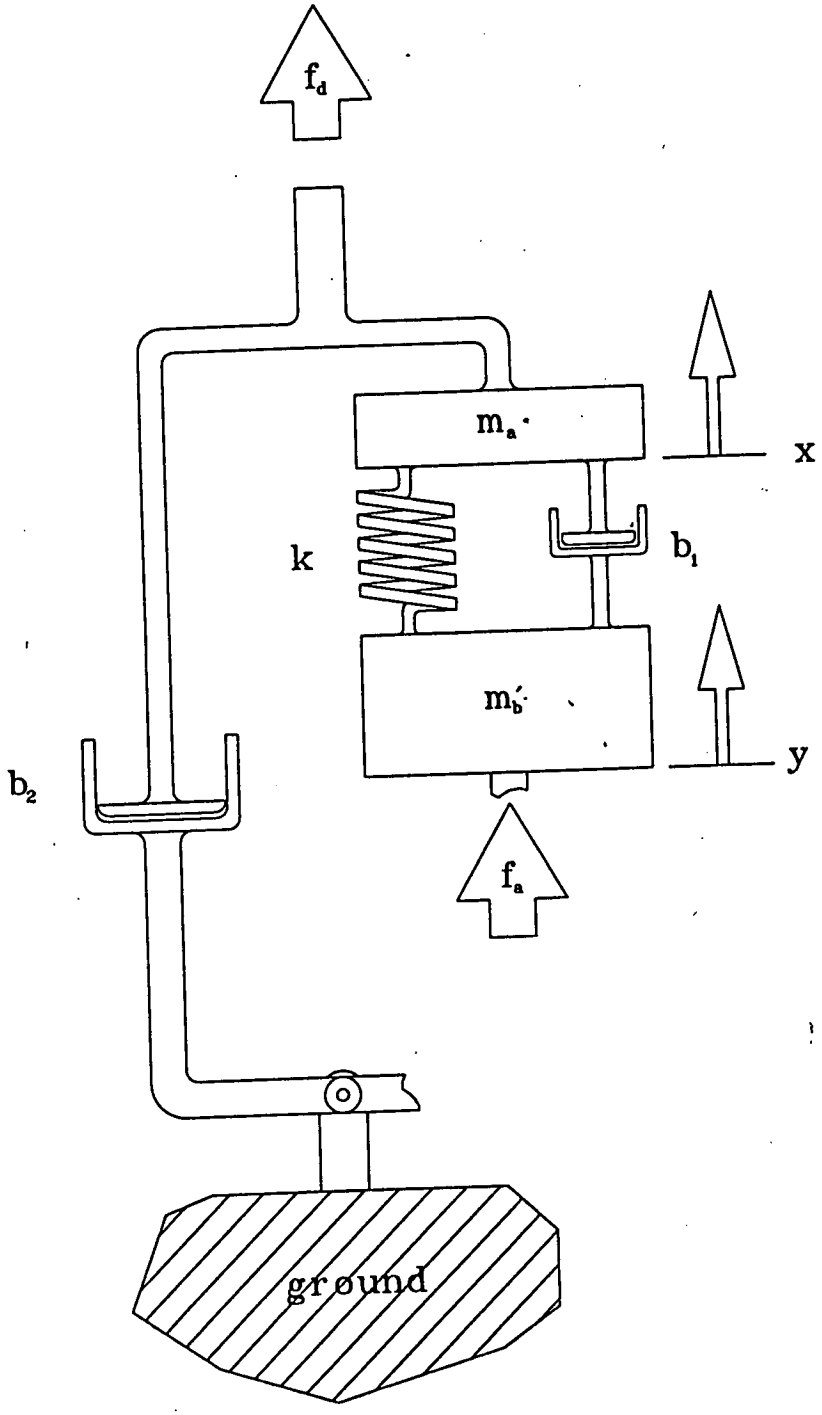

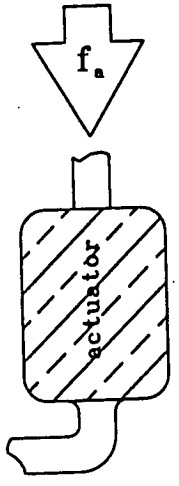

Figure 5.9:

m_b -- mass of nut portion of leg

J_s -- inertia of screw

J_m -- inertia of motor

g_s -- gear ratio of screw [L/rad]

g_h -- gear ratio of gearbox

$m_{b'}$ -- combined inertia of nut, screw, and motor seen at nut

k -- translational stiffness between nut and end of leg

b_1 -- translational damping between nut and end of leg (coupling)

b_2 -- translational damping between end of leg and ground (de-coupling)

α -- ratio $m_a/m_{b'}$

ζ_1 -- damping ratio for b_1 acting on m_a

ζ_2 -- damping ratio for b_2 acting on m_a

ζ_3 -- damping ratio for b_1 acting on $m_{b'}$

f_d -- disturbance force acting on m_a

f_a -- actuation force

e_a -- compensated actuation force (proportional, derivative)

e'_a -- compensated actuation force (lead network)

This analysis is separated into three major sections. The first analyzes the effect of the disturbing force (f_d) on the mass representing the platform (m_a) by deriving the transfer function $\dot{X}/F_d$. The effects are characterized using the dimensionless parameters α, ζ_1, and ζ_2, which represent the following:

α--the ratio of reflected platform mass (m_a) to reflected nut mass ($m_{b'}$)

ζ_1--the damping ratio for the coupling damper (b_1)

ζ_2--the damping ratio for the de-coupling damper (b_2).

It is concluded in Section V.C.1 that a little damping (ζ_2=0.15) prohibits the lower forcing function frequencies from causing an acceleration $\ddot{x}$ of m_a.

In Section V.C.2, the transfer function ($\dot{X}/F_a$) relating the actuation force (f_a) to the velocity $\dot{x}$ is derived. This transfer function is compared with $\dot{X}/F_d$ to show that without compensation, the disturbance force has better transmission characteristics. It is the purpose of Section V.C.3 to show that it is feasible that moderate compensation from a

control loop can make the actuation force have better transmission characteristics than the disturbance force over the entire frequency spectrum.

V.C.1. Derivation of $\dot{X}/F_d$ Transfer Function

1.1 Kinematics

The kinematic relation between motor and screw is given by

$$\dot{\theta}_m = g_h \, \theta_s . \tag{5.5}$$

And the kinematic relation between the screw and the nut is given by

$$\dot{\theta}_s = g_s \, \dot{y} . \tag{5.6}$$

1.2 Reflected Inertia

The inertia of the screw and motor as seen at m_b is designated as reflected inertia, $m_{b'}$, and is given by

$$m_{b'} = m_b + g_s^2 (J_s + g_h^2 \, J_m) , \tag{5.7}$$

1.3 Equations of Motion

Equation of motion for m_a is given by

$$f_d = m_a \ddot{x} + (b_1 + b_2) \, \dot{x} + k \, x - k \, y - b_1 \, \dot{y} . \tag{5.8}$$

Neglecting the actuation force, f_a, the equation of motion for m_b is given by

$$0 = m_{b'} \ddot{y} + b_1 \, \dot{y} + k \, y - k \, x - b_1 \, \dot{x} . \tag{5.9}$$

1.4 Laplace Domain

The Laplacian of (5.8) is

$$F_d(s) = (m_a s^2 + (b_1 + b_2) s + k) X(s) - (b_1 s + k) Y(s). \quad (5.10)$$

The Laplacian of (5.9) is

$$0 = (m_b s^2 + b_1 s + k) Y(s) - (b_1 s + k) X(s), \quad (5.11)$$

which yields the following function:

$$Y(s) = \frac{b_1 s + k}{m_b s^2 + b_1 s + k} X(s). \quad (5.12)$$

Substituting (5.12) into (5.10) and rearranging yields

$$F_d(s) = \left\{ \frac{(m_a s^2 + (b_1 + b_2) s + k)(m_b s^2 + b_1 s + k) - (b_1 s + k)^2}{m_b s^2 + b_1 s + k} \right\} X(s), \quad (5.13)$$

which when simplified yields

$$F_d(s) = \left\{ \frac{m_a m_b s^4 + (m_b (b_1 + b_2) + m_a b_1) s^3 + (k(m_a + m_b) + b_2 b_1) s^2 + (k b_2) s}{m_b s^2 + b_1 s + k} \right\} X(s). \quad (5.14)$$

This yields the desired transfer function:

$$\frac{\dot{X}(s)}{F_d(s)} = \frac{m_b s^2 + b_1 s + k}{m_a m_b s^3 + (m_b (b_1 + b_2) + m_a b_1) s^2 + (k(m_a + m_b) + b_1 b_2) s + (k b_2)}. \quad (5.15)$$

It is desirable to divide both numerator and denominator by $m_a m_b$, which yields

$$\frac{\dot{X}(s)}{F_d(s)} = \frac{\frac{1}{m_a} s^2 + \frac{b_1}{m_a m_b} s + \frac{k}{m_a m_b}}{s^3 + \left(\frac{(b_1 + b_2)}{m_a} + \frac{b_1}{m_b}\right) s^2 + \left(k\left(\frac{1}{m_a} + \frac{1}{m_b}\right) + \frac{b_1 b_2}{m_a m_b}\right) s + \frac{k b_2}{m_a m_b}}. \quad (5.16)$$

Now, the following natural frequencies are introduced:

$$\omega_a^2 = k / m_a, \qquad \omega_b^2 = k / m_b, \quad (5.17)$$

And the following damping relationships are introduced:

$$\zeta_1 = \frac{b_1}{2\sqrt{k\, m_a}}, \qquad \zeta_2 = \frac{b_2}{2\sqrt{k\, m_a}}, \qquad \zeta_3 = \frac{b_1}{2\sqrt{k\, m_{b'}}}. \tag{5.18}$$

Substituting into (16) gives the transfer function:

$$\frac{\dot{X}(s)}{F_d(s)} = \frac{\frac{1}{m_a} s^2 + \frac{2\,\zeta_1\,\omega_a}{m_{b'}} s + \frac{\omega_a^2}{m_{b'}}}{s^3 + 2((\zeta_1+\zeta_2)\,\omega_a+\zeta_3\omega_b)\,s^2 + (\omega_a^2+\omega_b^2+4\zeta_2\zeta_3\omega_a\omega_b)\,s + 2\zeta_2\omega_a\omega_b^2}. \tag{5.19}$$

The dimensionless parameter α is now introduced to relate the masses, damping ratios, and natural frequencies in the following manner:

$$m_a = \alpha\, m_{b'}, \qquad \zeta_3 = \sqrt{\alpha}\ \zeta_1, \qquad \omega_a = \omega_b / \sqrt{\alpha}\ . \tag{5.20}$$

Substitution of (5.20) into (5.19) yields the transfer function in its final form:

$$\frac{\dot{X}(s)}{F_d(s)} = \frac{G\,(s^2 + a_1\, s + a_0)}{s^3 + b_2\, s^2 + b_1\, s + b_0}, \tag{5.21}$$

where

$$G = \frac{1}{\alpha\, m_{b'}}$$
$$a_0 = \omega_b^2$$
$$a_1 = 2\,\zeta_1\,\sqrt{\alpha}\,\omega_b$$
$$b_0 = 2\,\zeta_2 / \sqrt{\alpha}\,\omega_b^3$$
$$b_1 = (1 + 1/\alpha + 4\,\zeta_1\,\zeta_2)\,\omega_b^2$$
$$b_2 = 2\,((1+\alpha)\,\zeta_1 + \zeta_2) / \sqrt{\alpha}\,\omega_b.$$

1.5 Frequency Response

Substitution of $s = -j\omega$ into (5.21) yields the following

$$\frac{\dot{X}(-j\omega)}{F_d(-j\omega)} = \frac{G\,((a_0 - \omega^2) + (-a_1\omega)j)}{((b_0 - b_2\omega^2) + (\omega^3 - b_1\omega)j)}, \tag{5.22}$$

whose magnitude is given by

$$\left\| \frac{\dot{X}(-j\omega)}{F_d(-j\omega)} \right\| = G \sqrt{\frac{(a_0 - \omega^2)^2 + (a_1\omega)^2}{(b_0 - b_2\omega^2)^2 + (\omega^3 - b_1\omega)^2}}, \tag{5.23}$$

and whose phase angle is given by

$$\left(\frac{\dot{X}(-j\omega)}{F_d(-j\omega)} \right) = \tan^{-1}\left(\frac{-a_1\omega}{a_0 - \omega^2} \right) - \tan^{-1}\left(\frac{\omega^3 - b_1\omega}{b_0 - b_2\omega^2} \right). \tag{5.24}$$

1.6 Discussion

Figure 5.10 illustrates the frequency response of the transfer function when there is no damping. Trial cases show (see Figure 5.11) that the b_1 damper reduces the dip in magnitude at frequency ratio 0.3, while the b_2 damper zeros the lower frequency lags and flattens the lower frequency magnitude. This shows that the disturbance force causes no acceleration at low frequencies. In other words, the damper b_2 dominates the relationship between x and f_d at low frequencies (below frequency ratio 1.0). At higher frequencies (above frequency ratio 1.0), the acceleration $\ddot{x}$ of the mass m_a again begins to dominate (as it did when there was no damping), but this time the dominance at the higher frequencies is desired because it is clearly an attenuation. What this means to the milling application is that significant effects of the milling cutter disturbance force are passively damped out by the de-coupling dampers in the legs.

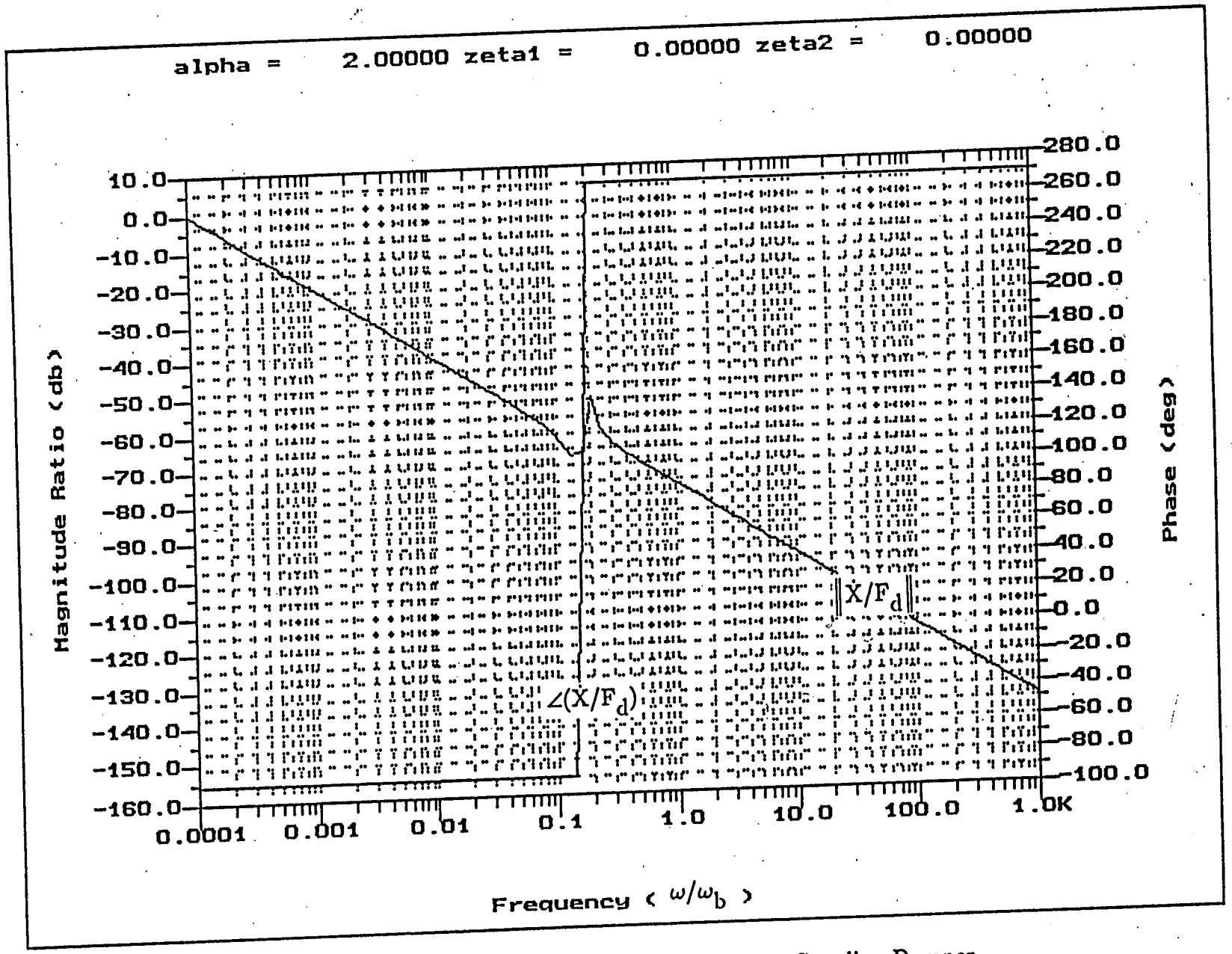

Figure 5.10: Frequency Response of $\dot{X}/F_d$ with No Dc-Coupling Damper

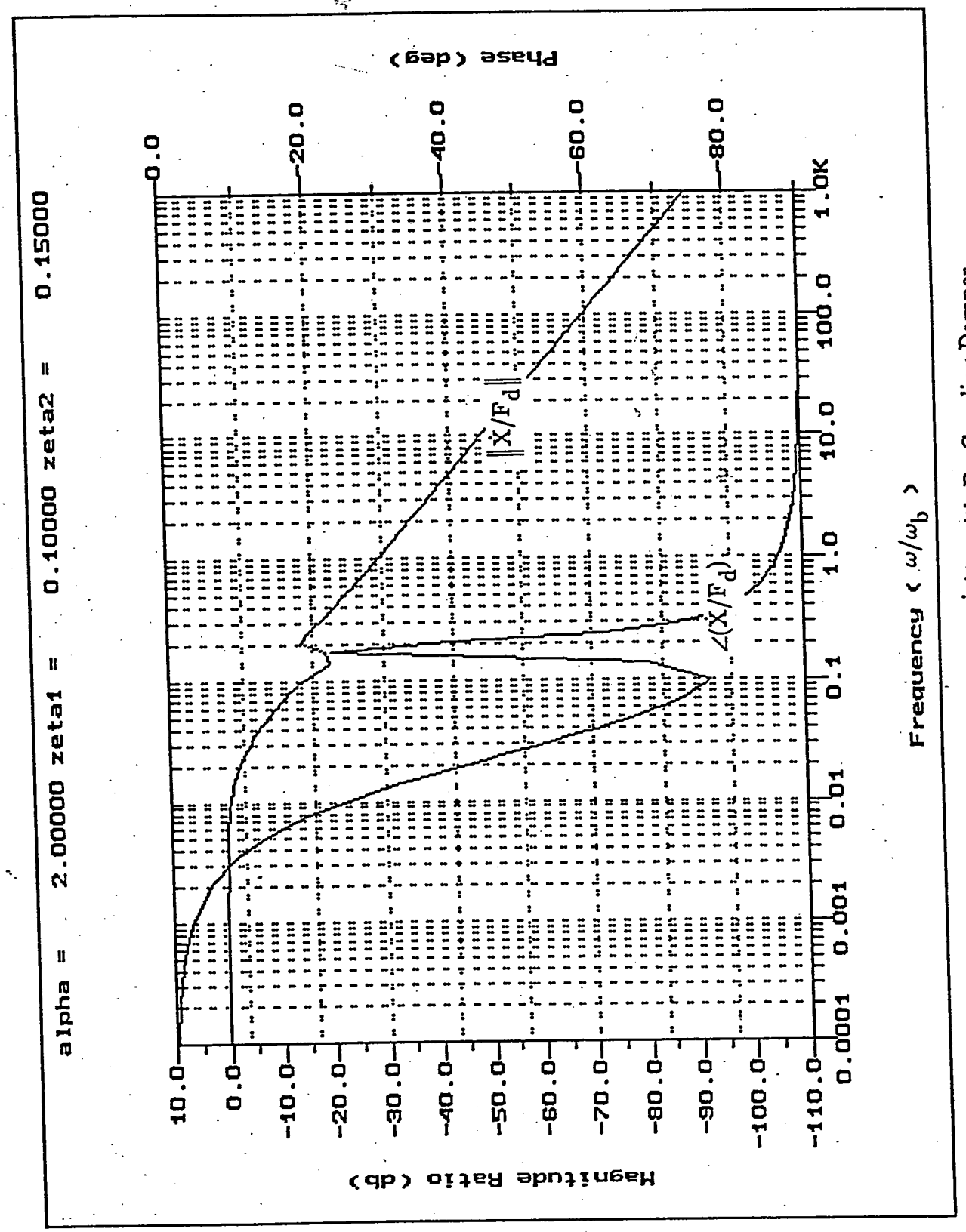

Figure 5.11: Frequency Response of $\dot{X}/F_d$ with De-Coupling Damper

2. Derivation of $\dot{X}/F_a$ Transfer Function

2.1 Equations of Motion

Neglecting the disturbance force f_d, the equation of motion for m_a is given by

$$0 = m_a \ddot{x} + (b_1 + b_2)\ \dot{x} + k\,x - k\,y - b_1\,\dot{y}. \tag{5.25}$$

And the equation of motion for m_b, is given by

$$f_a = m_b \ddot{y} + b_1\,\dot{y} + k\,y - k\,x - b_1\,\dot{x}. \tag{5.26}$$

2.2 Laplace Domain

The Laplacian of (5.25) is

$$0 = (m_a\,s^2 + (b_1 + b_2)\ s + k)\ X(s) - (b_1\,s + k)\ Y(s). \tag{5.27}$$

The Laplacian of (5.26) is

$$F_a(s) = (m_b\,s^2 + b_1\,s + k)\ Y(s) - (b_1\,s + k)\ X(s). \tag{5.28}$$

Simplifying (5.27) yields the following function:

$$Y(s) = \frac{m_a\,s^2 + (b_1 + b_2)\ s + k}{b_1\,s + k}\ X(s). \tag{5.29}$$

Substituting (5.29) into (5.28) and rearranging yields

$$F_a(s) = \frac{(m_b\,s^2 + b_1\,s + k)\ (m_a\,s^2 + (b_1 + b_2)\ s + k) - (b_1\,s + k)^2}{b_1\,s + k}\ X(s), \tag{5.30}$$

which when simplified yields

$$F_a(s) = \left\{\frac{m_a m_b\,s^4 + (m_b(b_1+b_2) + m_a b_1)\,s^3 + (k(m_a+m_b) + b_1 b_2)\,s^2 + (kb_2)\,s}{b_1\,s + k}\right\} X(s). \tag{5.31}$$

This yields the desired transfer function:

$$\frac{\dot{X}(s)}{F_a(s)} = \frac{b_1 s + k}{m_a m_b s^3 + (m_b(b_1+b_2) + m_a b_1) s^2 + (k(m_a+m_b) + b_1 b_2) s + (k b_2)} X(s). \quad (5.32)$$

which has the same denominator as $\dot{X}(s)/F_d(s)$. Dividing throughout by m_a m_b and re-arranging in terms of α, ζ_1, ζ_2, ω_b yields the following transfer function:

$$\frac{\dot{X}(s)}{F_a(s)} = \frac{G\ (c_1 s + c_0)}{s^3 + b_2 s^2 + b_1 s + b_0}, \quad (5.33)$$

where

$$G = \frac{1}{\alpha\ m_b},$$
$$c_0 = \omega_b^2$$
$$c_1 = 2\ \zeta_1 \sqrt{\alpha}\ \omega_b$$
$$b_0 = 2\ \zeta_2 / \sqrt{\alpha}\ \omega_b^3$$
$$b_1 = (1 + 1 / \alpha + 4\ \zeta_1 \zeta_2)\ \omega_b^2$$
$$b_2 = 2\ ((1 + \alpha)\ \zeta_1 + \zeta_2) / \sqrt{\alpha}\ \omega_b.$$

2.3 Discussion

Figure 5.12 shows the frequency response of the actuation force transfer function for the same design parameters taken in Section V.C.1. Figure 5.13 compares the two transfer functions to show that the disturbance force transfer function has better transmission characteristics at higher frequencies (above frequency ratio 1.0). It should be noted, however, that the actuation force is an uncompensated one. In other words, compensation due to an active control loop should be considered, so that the resulting compensated actuation force possesses better transmission characteristics than the disturbance force over the entire frequency spectrum. The analysis contained in the following section demonstrates that the compensated actuation forces in the legs of the platform can overcome a milling cutter disturbance force containing any frequency content to stabilize the lengths of the legs and hence the position and orientation of the workpiece.

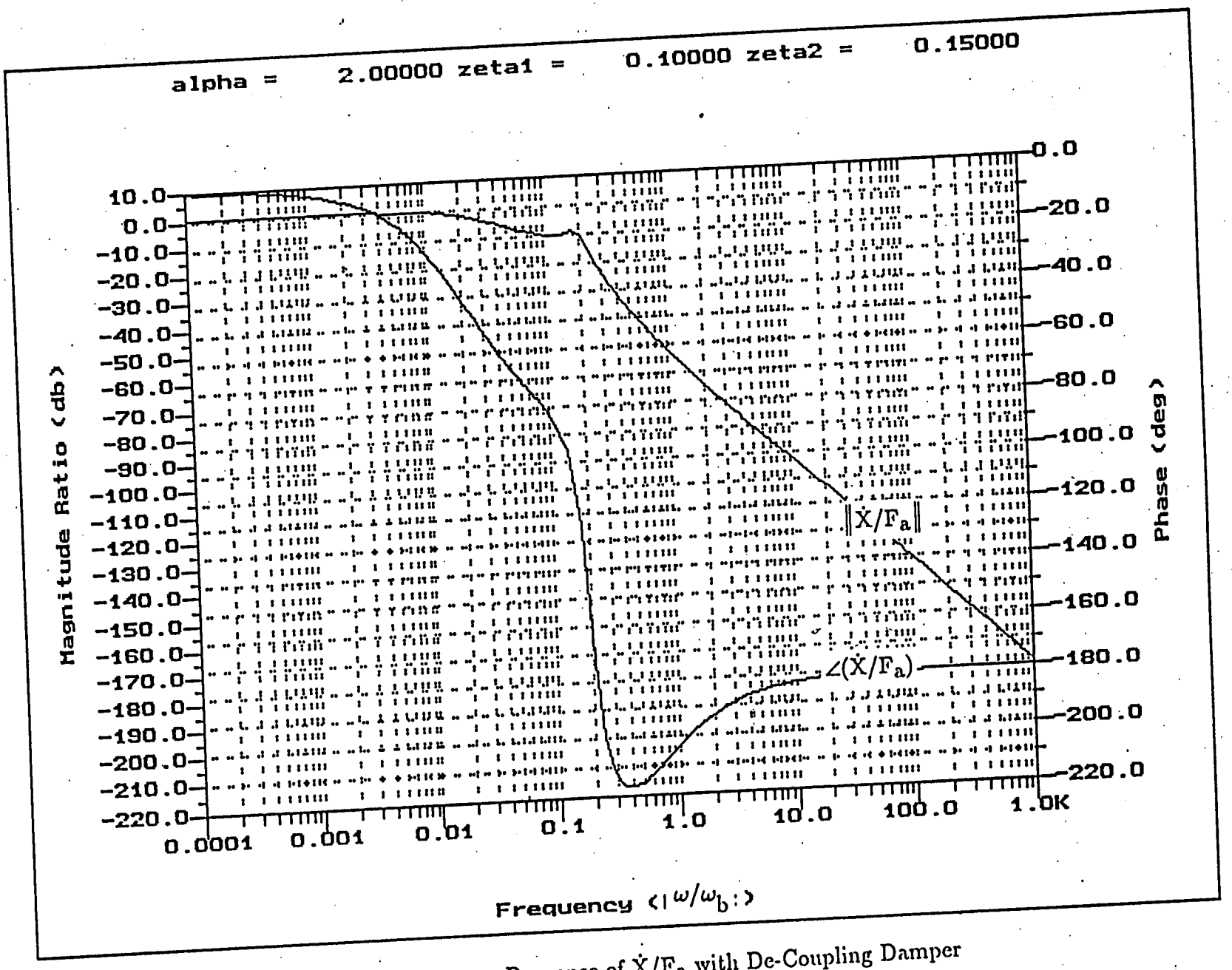

Figure 5.12: Frequency Response of $\dot{X}/F_a$ with De-Coupling Damper

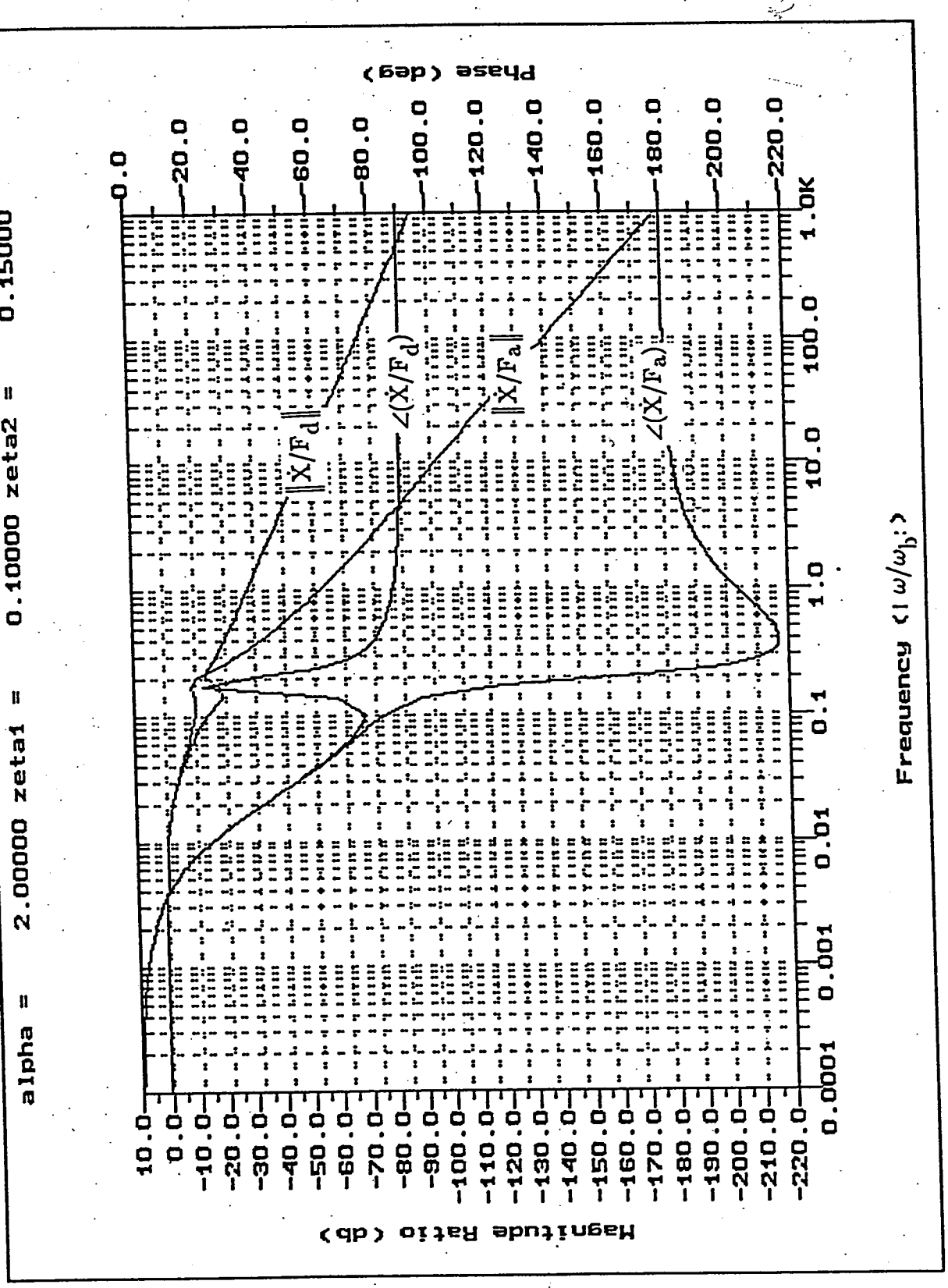

Figure 5.13: Frequency Response of $\dot{X}/F_a$ and $\dot{X}/F_d$ with De-Coupling Damper

3. Adding Compensation to the Actuation Force

3.1 Proportional and Derivative Gains

The following transfer function relates a control signal (e_a) to the actuation force:

$$\frac{F_a(s)}{E_a(s)} = K_p + K_d\, s, \tag{5.34}$$

where K_p is the proportional gain and K_d is the derivative gain. Multiplication by (5.33) yields the desired transfer function $\dot{X}/E_a$.

Figures 5.14, 5.15, and 5.16 demonstrate the desirable effect that this transfer function has in comparison with $\dot{X}/F_d$. (The same design parameters α, ζ_1, and ζ_2 from Sections C.1 and C.2 were used.) In magnitude, the compensated actuation force e_a outperforms the disturbance force f_d over all frequencies. A slight lag does, however, exist near frequency ratio 1.0.

3.2 Lead Network

The following transfer function relates a modified control signal (e'_a) to the actuation force:

$$\frac{F_a(s)}{E'_a(s)} = K_p\, \frac{1 + \tau_1 s}{1 + \tau_2 s}, \tag{5.35}$$

where τ_1 and τ_2 are the lead constants. Multiplication by (5.33) yields the desired transfer function $\dot{X}/E'_a$.

Figure 5.17 demonstrates that the above actuation force outperforms the disturbance force over all frequencies in both magnitude and phase. This means that the compensated actuation force e'_a can overcome a disturbance force f_d at any frequency to stabilize the mass m_a.

It is interesting to note what happens to the above compensated actuation force when the de-coupling damper is omitted ($\zeta_2 = 0$). Figure 5.18 demonstrates that the disturbance force will now outperform it. With no de-coupling damper, the compensated actuation force must be magnified by at least 45 db, which is a factor of about 100.

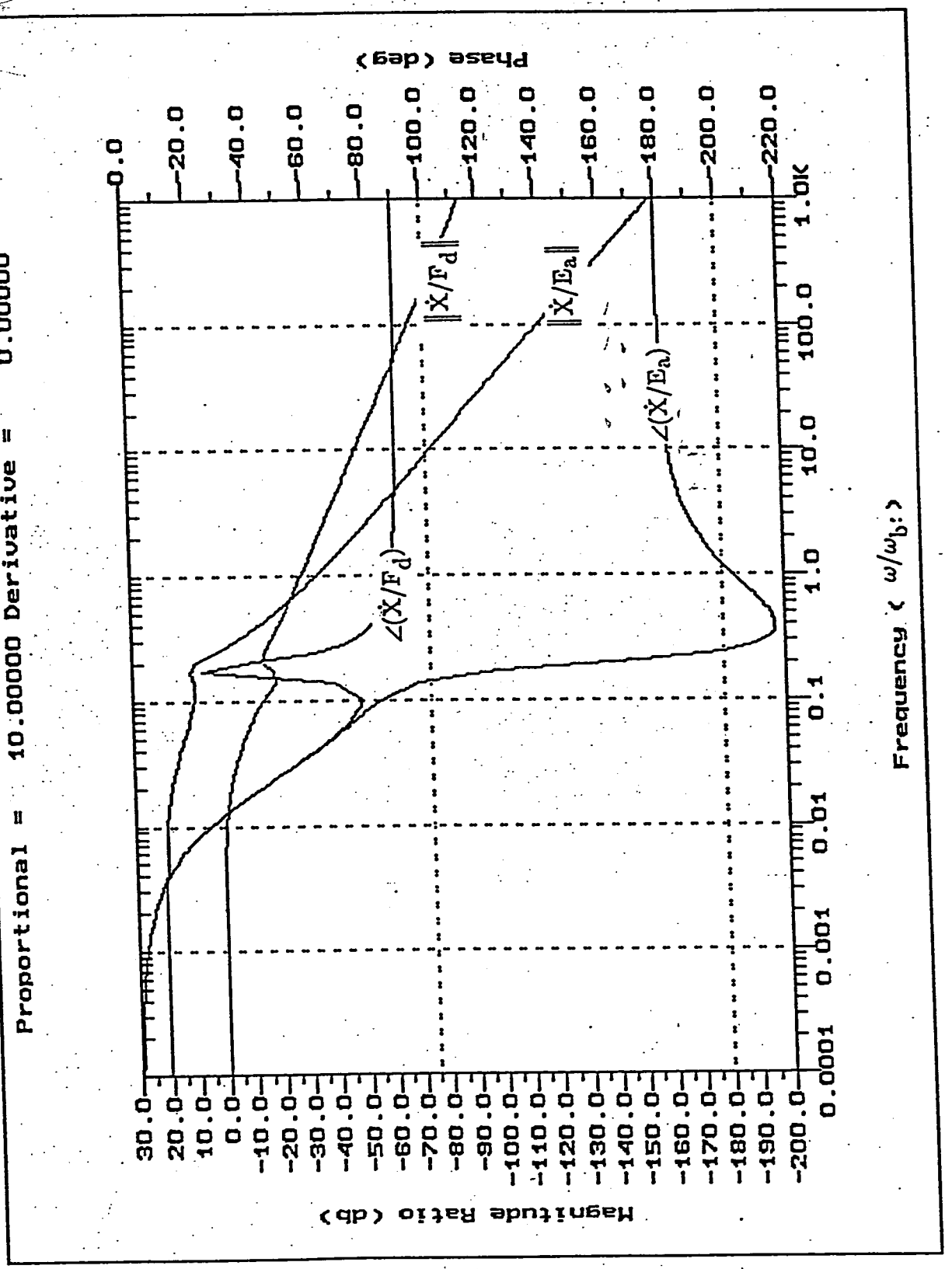

Figure 5.14: Effect of Proportional Gain on $\dot{X}/F_a$.

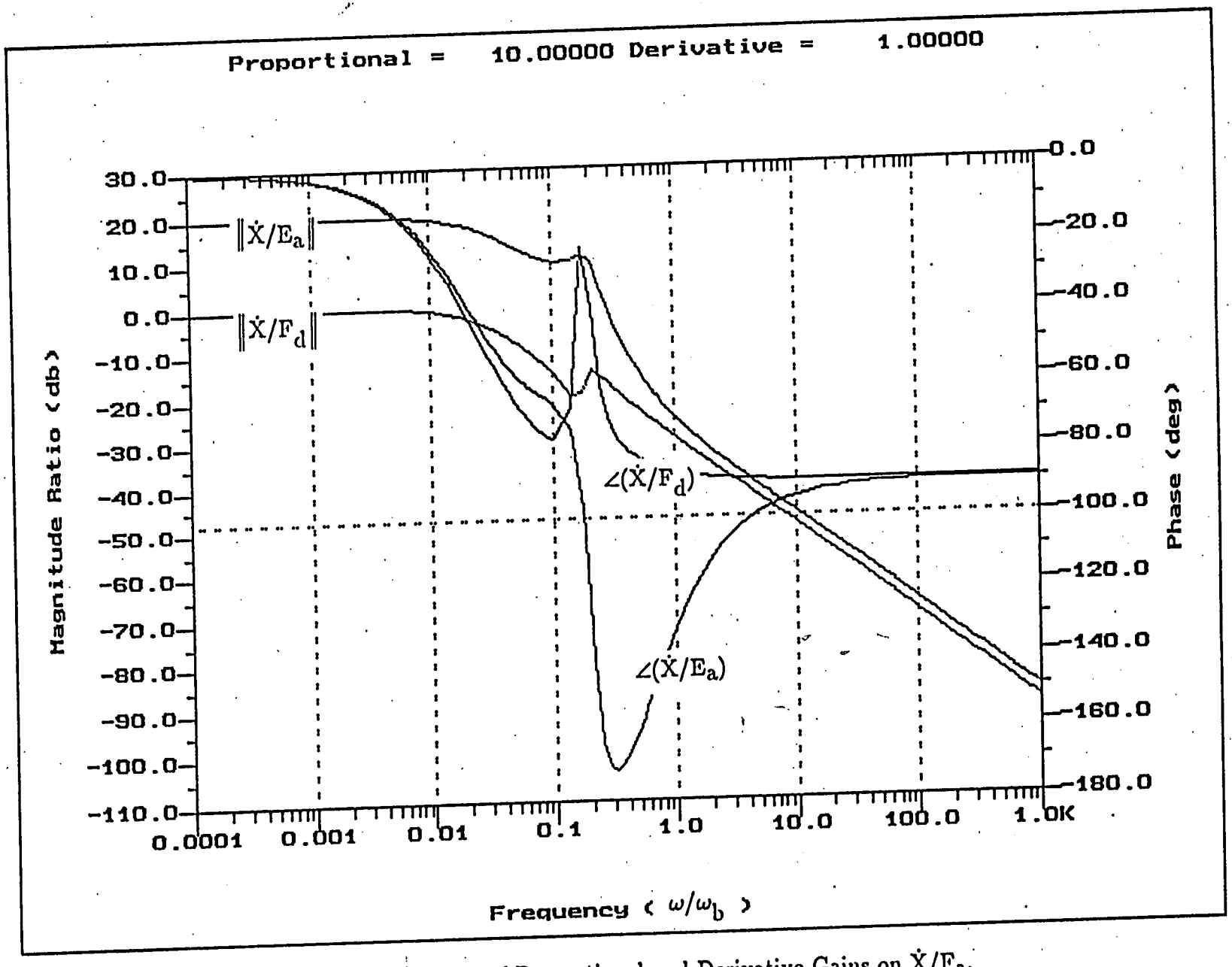

Figure 5.15: Effect of Proportional and Derivative Gains on $\dot{X}/F_a$.

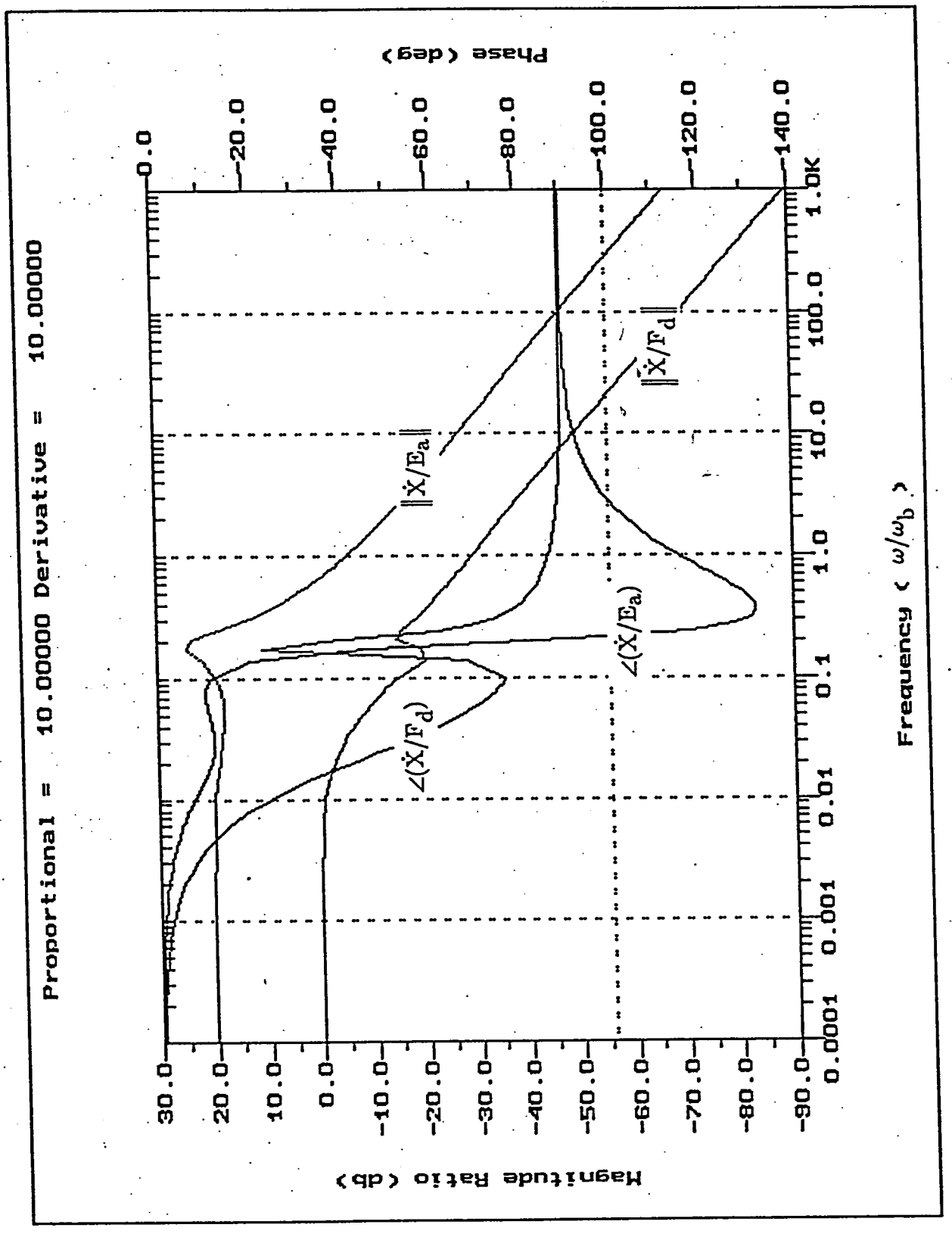

Figure 5.16: Effect of Proportional and Derivative Gains on $\dot{X}/F_a$.

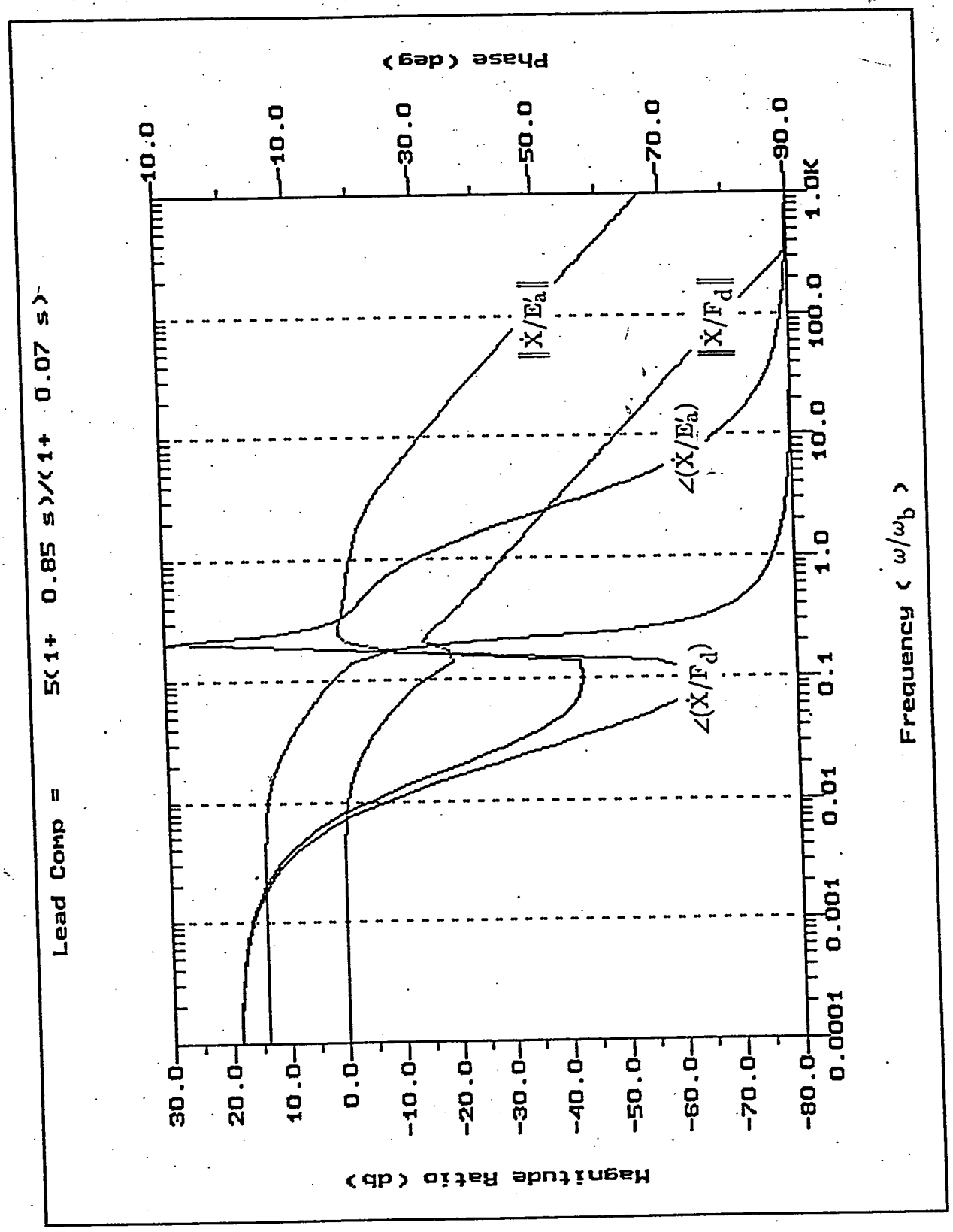

Figure 5.17: Effect of Phase Lead on $\dot{X}/F_a$.

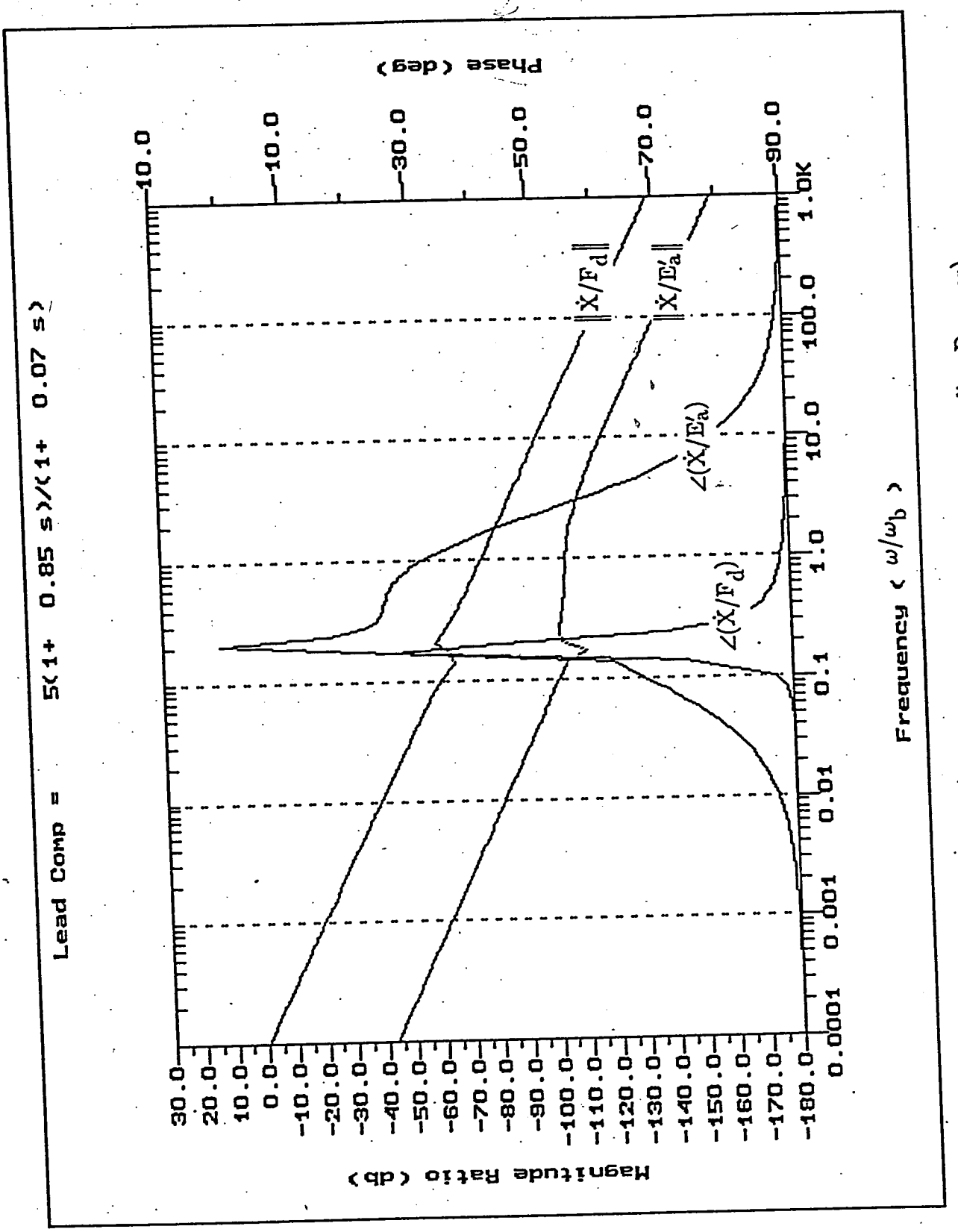

Figure 5.18: Effect of Phase Lead on $\dot{X}/F_a$ (with no De-Coupling Damper).

VI. Computer Graphics Animation

A computer graphics animation of the KP performing machining operations was prepared on a Silicon Graphics Crimson workstation. The animation software was developed using a combination of in-house written C language code together with the Silicon Graphics Inventor software and the Motif development system.

The development of the animation consisted of four tasks. First, a three dimensional model of the Bridgestone 2 axis mill was prepared. The animated mill was developed from this model. Second, a parametric model of the KP was developed. This parametric model allows for each part of the KP to be resized. The animation code is simply recompiled whenever the KP dimensions change. Third, kinematic control software was written which calculates the joint angles and slider lengths for each of the legs of the KP when given the desired position and orientation of the top platform relative to the base platform. This control software utilizes the parametric symbols for the KP so that it does not have to be rewritten when the KP dimensions change. Fourth, software was written which generates a tool path for a cutting operation. The tool path generation software was written assuming that the shell shown in Figure 4.3 was being manufactured.

Images from the resulting animation are shown in Figures 6.1 through 6.4. End milling is being performed in Figures 6.1 and 6.2 in order to remove material from the top of the original workpiece (the original rectangular workpiece is shown as transparent in Figure 6.1). Ball milling is shown in Figures 6.3 and 6.4. It is during this operation that the final contoured surfaces of the shell are fabricated.

A video of the animation was prepared and delivered with this report. The video shows end milling and ball milling operations and demonstrates the ability of the KP to position and orient the workpiece relative to the milling tool as required.

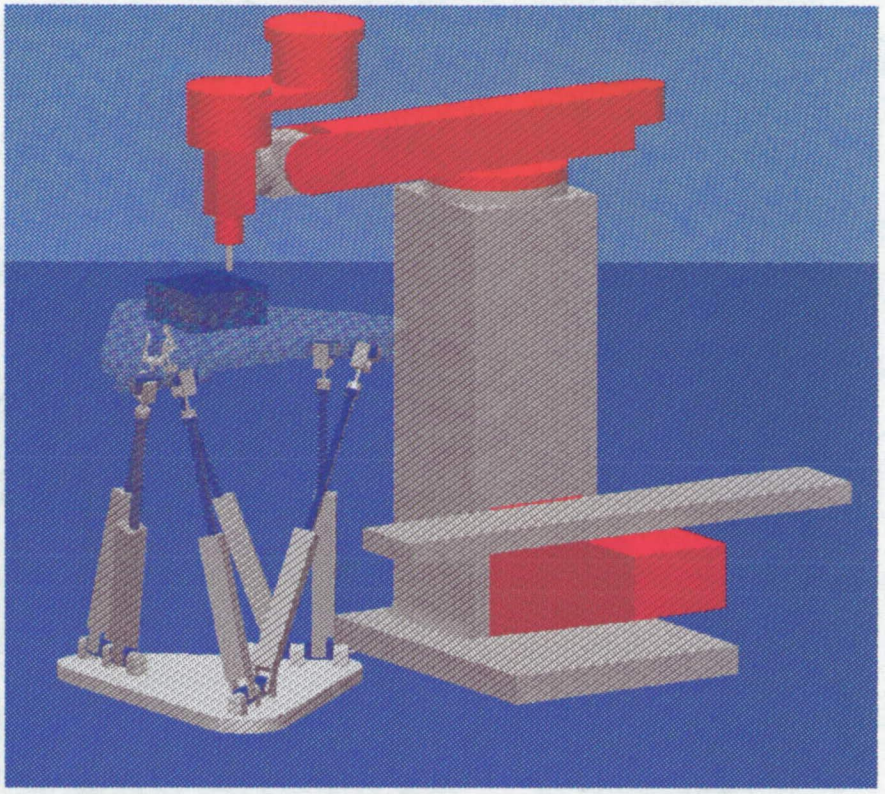

Figure 6.1: End Milling

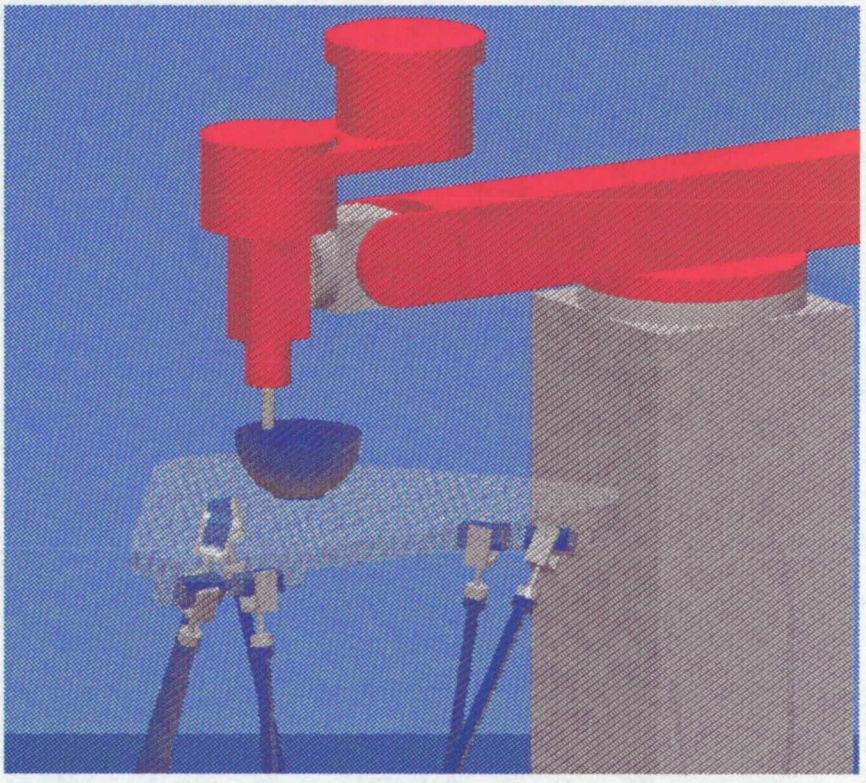

Figure 6.2: End Milling

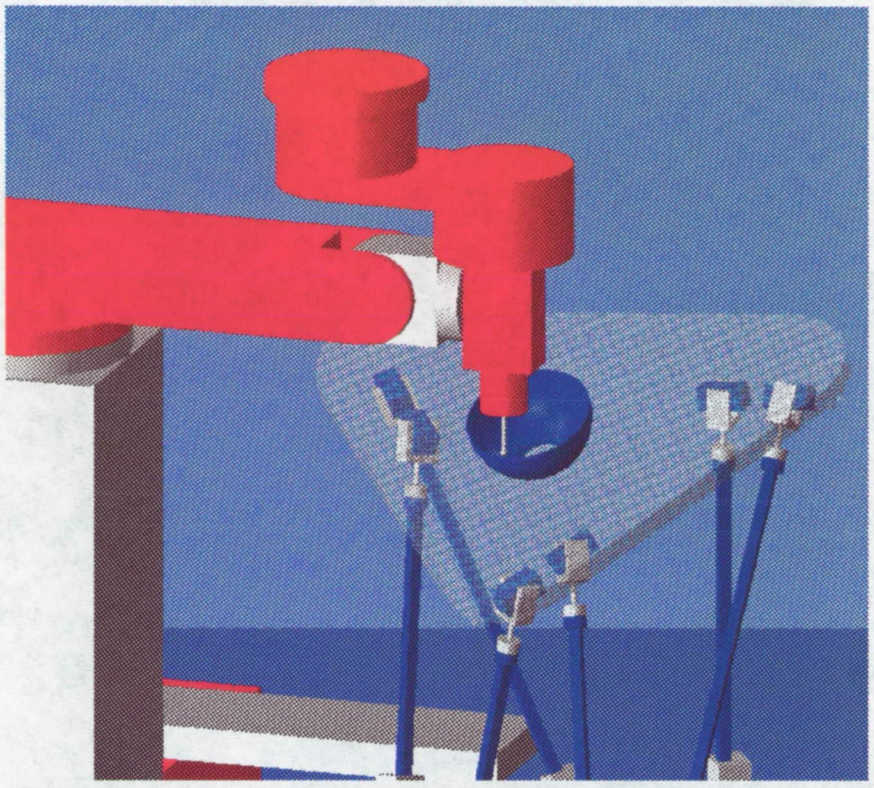

Figure 6.3: Ball Milling

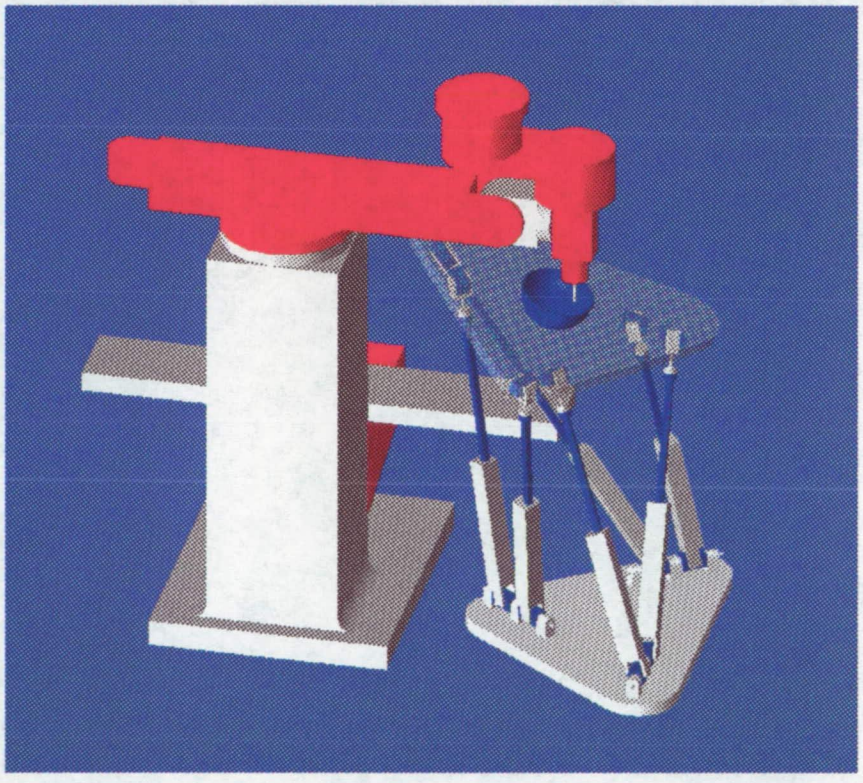

Figure 6.4: Ball Milling

VII. Conclusions

All the tasks defined for Phase I have been successfully accomplished. Specifically,

(1) A machining task for the Kinestatic Platform was identified which will lead to considerable savings in manufacturing shuttle parts. Equally important, a test bed in the Rockwell Logistics Center is being established which will permit NASA, Rockwell, and the University of Florida to develop and commercialize this new technology.

(2) Kinematic, static, and dynamic analyses for the platform have been performed which demonstrate that the task of milling light aluminum parts is achievable.

(3) These same kinematic, static, and dynamic analyses will be used in Phase II to determine all necessary parameters to obtain an optimal KP to perform the milling tasks.

(4) The kinematic and static analyses have been used to produce a graphic animation of the KP as it performs a milling operation.

(5) In parallel with the above developments, specific NASA applications where the KP technology can be applied were identified and listed.

An active/passive scheme has been demonstrated that facilitates the stable control of the position and orientation of the workpiece of the kinestatic platform by eliminating chatter between the milling cutter and the workpiece which is to be machined. The de-coupling damper incorporated in the legs together with moderate amounts of leg compliance constitute the passive elements. It was shown how the passive elements work in harmony with the active elements, which are compensated actuation forces in the legs, to attenuate the disturbance forces applied by the milling cutter.

It is our contention that the success of the first phase of this project has established an appropriate point of departure for the phase 2 activity. In anticipation of the second phase, we encourage, solicit, and welcome any criticisms or recommendations from all levels of engineering personnel as well as all management levels at NASA/KSC. It is further our intent to present the practical application of advanced technology toward the continued unqualified success of this project.

VIII. References

[1] M. Griffis and J. Duffy, "A Forward Displacement Analysis of a Class of Stewart Platforms," Journal of Robotic Systems, Vol. 6, No. 6, 1989, pp.703-720.

[2] D. Stewart, "A Platform With Six Degrees of Freedom," Proc. Inst. Mech. Eng., London, Volume 180, 1965, pp. 371-386.

[3] C. Innocenti and V. Parenti-Castelli, "Closed form Position Analysis of a 5-5 Parallel Mechanism," Transactions of ASME Journal of Mechanical Design (in press), Appeared in Proceedings of 1990 Biennial ASME Mechanisms Conference (Chicago).

[4] M. Griffis and J. Duffy, "Kinestatic Control: A Novel Theory for Simultaneously Regulating Force and Displacement," Transactions ASME Journal of Mechanical Design, 1991, (Best Paper Award at the 21st Biennial Mechanisms Conference, Chicago).

[5] M. Griffis and J. Duffy, "On a General Model of Spatial Stiffness," Best Paper Award at the VIII CISM-IFToMM Symposium "Ro.man.sys '90", Cracow, Poland.